

Ring-opening polymerization of *rac*-lactide mediated by tetrametallic lithium and sodium amine-bis(phenolate) complexes

Dalal Alhashmialameer,^a Nduka Ikpo,^a Julie Collins,^b Louise N. Dawe,^{abc} Karen Hattenhauer,^a and Francesca M. Kerton^{*a}

^a Department of Chemistry, Memorial University of Newfoundland, St. John's, Newfoundland, Canada A1B 3X7. E-mail: fkerton@mun.ca

^b C-CART X-ray Diffraction Laboratory, Memorial University of Newfoundland, St. John's, Newfoundland, Canada

^c Current Address: Department of Chemistry, Wilfrid Laurier University, Waterloo, Ontario, Canada

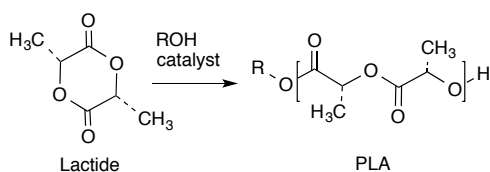
† Electronic supplementary information (ESI) available. For ESI data in and other electronic format see DOI:

Abstract

Lithium and sodium compounds supported by tetradentate amino-bis(phenolato) ligands, $[\text{Li}_2(\text{N}_2\text{O}_2^{\text{BuBuPip}})]$ (**1**), $[\text{Na}_2(\text{N}_2\text{O}_2^{\text{BuBuPip}})]$ (**2**) (where $[\text{N}_2\text{O}_2^{\text{BuBuPip}}] = 2,2'\text{-}N,N'\text{-homopiperazinyl-bis(2-methylene-4,6-}t\text{-tert-butylphenol)}$), and $[\text{Li}_2(\text{N}_2\text{O}_2^{\text{BuMePip}})]$ (**3**), $[\text{Na}_2(\text{N}_2\text{O}_2^{\text{BuMePip}})]$ (**4**) (where $[\text{N}_2\text{O}_2^{\text{BuMePip}}] = 2,2'\text{-}N,N'\text{-homopiperazinyl-bis(2-methylene-4-methyl-6-}t\text{-tert-butylphenol)}$) were synthesized and characterized by NMR spectroscopy and MALDI-TOF mass spectrometry. Variable temperature NMR experiments were performed to understand solution-phase dynamics. The solid-state structures of **1** and **4** were determined by X-ray diffraction and reveal tetrametallic species. PGSE NMR spectroscopic data suggests that **1** maintains its aggregated structure in CD_2Cl_2 . The complexes exhibit good activity for controlled ring-opening polymerization of *rac*-lactide (LA) both solvent free and in solution to yield PLA with low dispersities. Stoichiometric reactions suggest that the formation of PLA may proceed by the typical coordination-insertion mechanism. For example, ^7Li NMR experiments show growth of a new resonance when **1** is mixed with 1 equiv. LA.

Introduction

In recent years, considerable attention has been directed toward the design of bio-based and degradable polymers, particularly linear aliphatic polyesters such as polylactide (PLA) and polycaprolactone (PCL).¹⁻³ PLA has received a significant amount of interest industrially as a packing material and in the pharmaceutical and biomedical fields⁴⁻¹⁴ because it is biodegradable, biocompatible and can be synthesized from renewable feedstocks. An equally important aspect of PLA is its unique physical properties, which make it a viable alternative to more traditional polymers, like polystyrene and polyethylene terephthalate for containers including bottles.^{7, 8, 12} In the synthesis of PLA, to achieve a high degree of control (including a high molecular weight with a low dispersity), ring opening polymerization (ROP) of lactide (LA) with an initiator/catalyst is the ideal route (Scheme 1).¹⁴



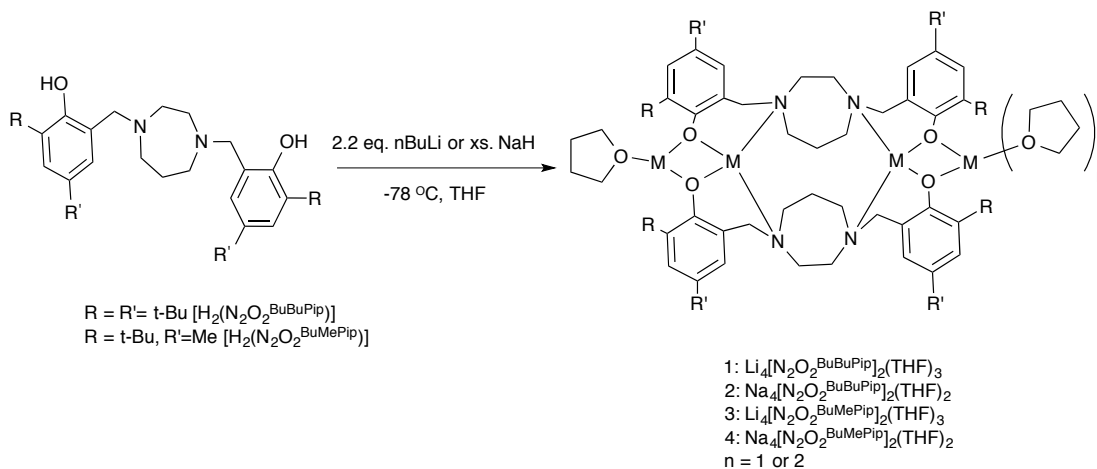
Scheme 1. Synthesis of polylactide by ROP route.

Ligands with *N*- and *O*-donor atoms such as aminephenolates have become an important ligand class in this field due to their ability to coordinate to a wide range of metal centers. Variation of the steric properties of the ligand is also readily achieved by changing either the backbone and/or the phenolate substituent.¹⁵ To initiate the polymerization of lactide and ϵ -caprolactone, main group metals are often employed with these ligands: magnesium,¹⁶⁻²⁶ calcium,^{16, 26, 27} barium,²⁸ aluminum have all been used.²⁹⁻³⁴ In addition, alkali metals such as lithium^{26, 25-48} and sodium^{26, 38, 47-51} bearing bulky ligands have shown promise in ROP of cyclic esters with few side reactions. Both metals tend to form aggregates in solution and in the crystalline state depending on the steric properties of the ligand or solvent used.^{35-49, 51} These complexes are attractive in this field because of their stability, low cost and toxicity. The current work targets the preparation of a series of multinuclear lithium and sodium complexes and subsequent investigation of their catalytic activity in the ROP of *rac*-lactide, both solvent free and in solution, in the presence and absence of benzyl alcohol.

Results and discussion

Synthesis and characterization of ligands, lithium and sodium complexes

The tetradentate amine-bis(phenol) ligands were synthesized via a modified Mannich condensation reaction in water.⁵² These and closely related ligands have previously been used to prepare complexes of Ti,⁵³⁻⁵⁶ Mn,⁵⁷ Al,⁵⁸ Zr and Hf,⁵⁹ Mo,⁶⁰ and Fe.⁶¹⁻⁶³ As shown in Scheme 2, lithium complexes with the formulation $(\text{Li}_2\text{O}_2\text{N}_2^{\text{BuBuPip}})_2(\text{THF})_3$ and $(\text{Li}_2\text{O}_2\text{N}_2^{\text{BuMePip}})_2(\text{THF})_3$ were synthesized by the reaction of $\text{H}_2[\text{O}_2\text{N}_2]^{\text{BuBuPip}}$ and $\text{H}_2[\text{O}_2\text{N}_2]^{\text{BuMePip}}$ with 2.2 equivalents of *n*-BuLi in THF. Tetranuclear sodium complexes were produced by reacting the appropriate ligand with an excess of NaH as shown in Scheme 2. The complexes were characterized using MALDI-TOF MS and ¹H, ¹³C and ⁷Li NMR spectroscopies. The structures of **1** and **4** were determined via single crystal X-ray diffraction analysis. Unfortunately, elemental analyses gave consistently lower than expected carbon values across all samples, which may be indicative of incomplete combustion. Although for the Li complexes, it may also suggest contamination with lithium oxide impurities.



Scheme 2. Synthesis of lithium and sodium complexes.

Crystal Structure Determination

For complex **1**, crystals suitable for single crystal X-ray diffraction were formed by slow evaporation of a toluene/pentane solution under an inert atmosphere at -35 °C. The ORTEP structure of complex **1** ($\{\text{Li}_2[\text{N}_2\text{O}_2^{\text{BuBuPip}}]\}_2 \cdot 3\text{THF}$) is shown in Figure 1 and the crystallographic

data are collected in Table S1. The compound contains four Li atoms, capped by two amine-bis(phenolate) ligands. At its core, only three of the four Li centers are tetracoordinate, with the fourth being tricoordinate. Selected bond lengths (Å) and angles (°) for compound **1** are presented in Table S2. Two terminal lithium centers Li(1) and Li(4) are bonded to two phenolate oxygen atoms (Li(1)-O(1), 1.804 Å, Li(1)-O(3), 1.848 Å, Li(4)-O(2), 1.899 Å, Li(4)-O(4) 1.922 Å) with distances in agreement to those reported by Chen *et al.* for a series of tetranuclear ladder-like lithium phenolates,⁴¹ and other similar species.^{35, 44} The terminal Li atoms are bound by one or two THF molecules (Li(1)-O(5), 1.934 Å, Li(4)-O(7), 2.085 Å, Li(4)-O(6) 2.009 Å) resulting in pseudo-trigonal planar (Li(1)) and tetrahedral (Li(4)) coordination environments. Each central Li atom is bound by two N atoms and bridging phenolate O atoms. Li-O and Li-N bond lengths are in good agreement with previously observed literature values for similar systems.⁴¹⁻⁴² Each of these lithium atoms interacts weakly with an adjacent terminal lithium atom (Li(1)-Li(2), 2.493 Å, Li(3)-Li(4), 2.583 Å) and agrees with the values reported by Chen *et al.* for analogous Li-containing compounds (2.403(7)-2.444(4) Å).^{35, 41}

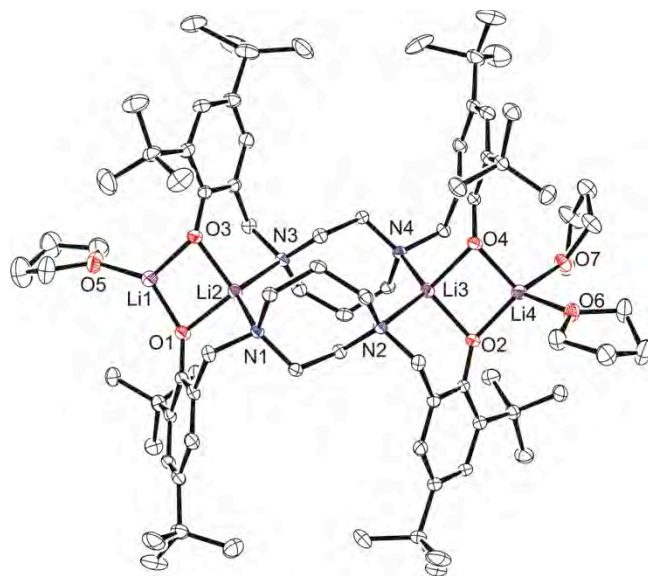


Figure 1. Molecular structure (ORTEP) and partial numbering scheme for **1**. Ellipsoids are shown at the 50% probability level (H-atoms omitted for clarity).

Colorless crystals of complex **4** were collected upon recrystallization in toluene/pentane under an inert atmosphere at -35 °C. The molecular structure of complex **4**

($\{\text{Na}_2[\text{N}_2\text{O}_2^{\text{BuMePip}}]\}_2 \cdot 2\text{THF}$) is shown in Figure 2 and the crystallographic parameters are given in Table S1. The arrangement of the metal centers is different to compound **1** due to the larger size of sodium compared to lithium. Complex **4** is dimeric with the sodium atoms forming a tetranuclear node, THF molecules are bonded to the terminal sodium atoms in a symmetric arrangement. A simplified illustration of the bonding in **4** is shown in Figure 3. Two sodium atoms Na(1) and Na(3) form a rhomboid structure with two bridging phenolate oxygen donors, O(1) and O(4). Atoms Na(1) and Na(3) are each five coordinate and bonded to both the amine nitrogen atoms and the other phenolate oxygen donors of the tetradentate ligand. Selected bond lengths (Å) and angles (°) for compound **4** are presented in Table S2. According to the calculated tau parameter ($\tau = (\beta - \alpha)/60$), the geometry around the inner sodium centers can be described as distorted square pyramidal.⁶⁴⁻⁶⁷ The τ value is close to 0, as β the largest angle is $139.96(5)^\circ$ and α the second largest angle in the coordination sphere is $134.44(5)^\circ$ as shown in Figure 3b. A Na(1)-Na(3) interatomic distance of 3.3769 \AA is observed which is within the typical range observed for related complexes.⁴⁹ In comparison to the bonding observed in **1**, the bond distances for Na(1)-O(4), Na(1)-O(1), Na(1)-N(1) and Na(1)-N(2) are as expected longer $2.3957(13)$, $2.3450(14)$, $2.6761(16)$ and $2.6392(16) \text{ \AA}$. All values are in statistical agreement with previously observed related bond distances in the literature.^{38, 47-48, 50-51} The phenyl rings of the ligand display π interactions with the outer sodium atoms and this is attributed to the flexibility of the aromatic rings to bend toward the metal centers. The Na-C π bond is supported by the short distances between the sodium and carbon atoms, with Na(2)-C(21), Na(2)-C(26), Na(2)-C(8), Na(2)-C(7) bond distances of $2.6683(18)$, $2.7093(19)$, $2.8526(19)$, $2.8788(19) \text{ \AA}$, respectively. These are comparable to those reported in previous studies.^{38, 50-51}

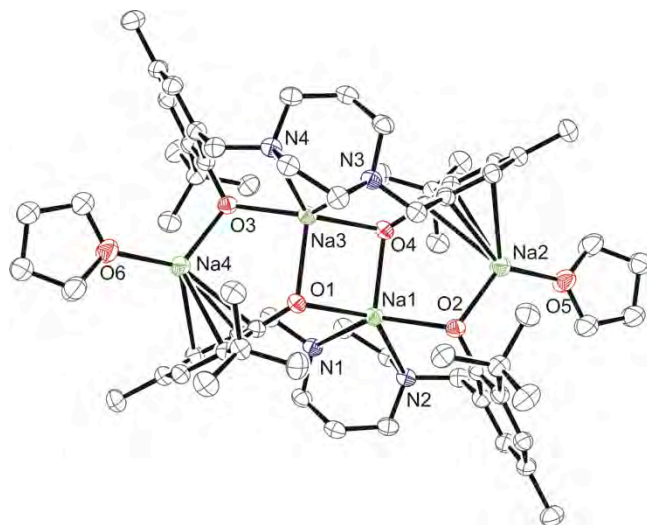


Figure 2. Molecular structure (ORTEP) and partial numbering scheme for **4**. Ellipsoids are shown at the 50% probability level (H-atoms omitted for clarity).

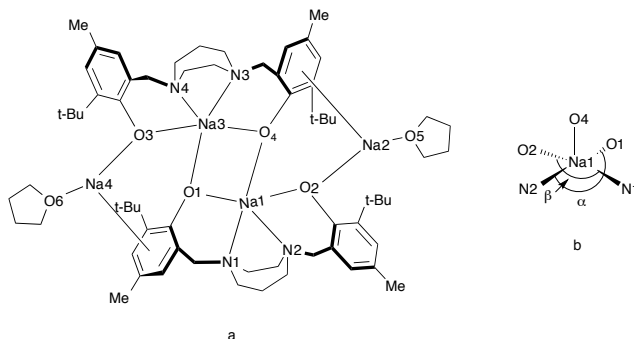


Figure 3. [a] Schematic representation of **4**. [b] Representation of the five-coordinate environment of Na(1).

Solution-state NMR Spectroscopy

The solution structures of complexes **1**, **2**, **3** and **4** in C_6D_6 and C_5D_5N were investigated by 1H and, where appropriate, 7Li NMR spectroscopy. For complexes **1** and **2** in C_6D_6 at 298 K, only one set of $ArCH_2$, *t*-Bu and homopiperazine (CH_2) resonances are observed, which is indicative of a centrosymmetric species (Figure S1). We assumed that disaggregation might be occurring as a result of steric crowding/congestion, wherein the structure of the ligand causes the degree of Li-O aggregation to be less in solution than the solid-state. The dissociation behavior of related tetranuclear lithium compounds in C_6D_6 and C_5D_5N at 296.2 K has previously been noted by others^{35, 44} in which ladder complexes undergo dissociation in solution rather than

remaining intact.

To further study the aggregation behavior of complex **1**, variable-temperature (VT) ^1H and ^7Li NMR spectra were obtained in $\text{C}_5\text{D}_5\text{N}$ from 233 to 318 K (shown in Figure 4 and 5, respectively). At room temperature, the proton resonances are noticeably sharper in $\text{C}_5\text{D}_5\text{N}$ compared to those seen in C_6D_6 (Figure S2), suggesting that the pyridine preferentially coordinates to the metal center and reduces fluxionality in the complexes.

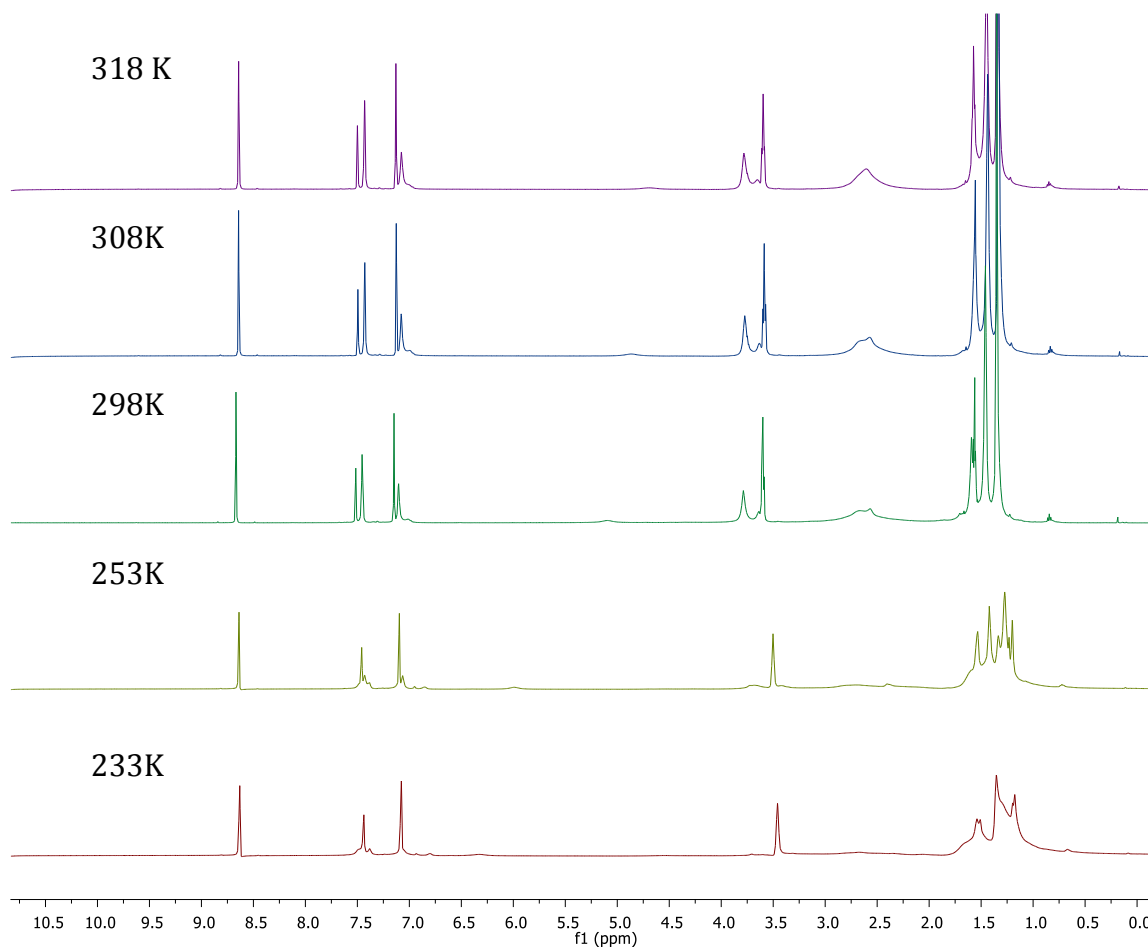


Figure 4. VT ^1H NMR spectrum (500 MHz, $\text{C}_5\text{D}_5\text{N}$) of **1**.

As seen in Figure 5, at room temperature and above, the ^7Li NMR spectra display a single peak at approximately 3.8 ppm ($\omega_{1/2} = 29.6$ Hz), corresponding to a single type of lithium environment, which contrasts with the solid-state structure where two environments are present. However, at low temperature (233 K) four Li environments were observed at 4.0 ($\omega_{1/2} = 70.6$ Hz), 3.8 ($\omega_{1/2} = 10.01$ Hz), 3.6 ($\omega_{1/2} = 27.2$ Hz) and 3.3 ($\omega_{1/2} = 94.5$ Hz) ppm. Our results contrast with the

previously reported work by Kozak³⁵ and Chen⁴¹ groups, who observed symmetric Li environments for similar complexes. This unique observation is likely because at low temperatures the tetralithium adduct is the dominant species present. On going from 233 K to 333 K, a small change in the chemical shift was observed which is consistent with those reported for other Li-based phenolates.^{35, 41} ⁷Li NMR spectra were also obtained in the formally non-coordinating solvent deuterated benzene. As expected, a major lithium environment at lower frequency, 1.58 ppm (Figure S4).

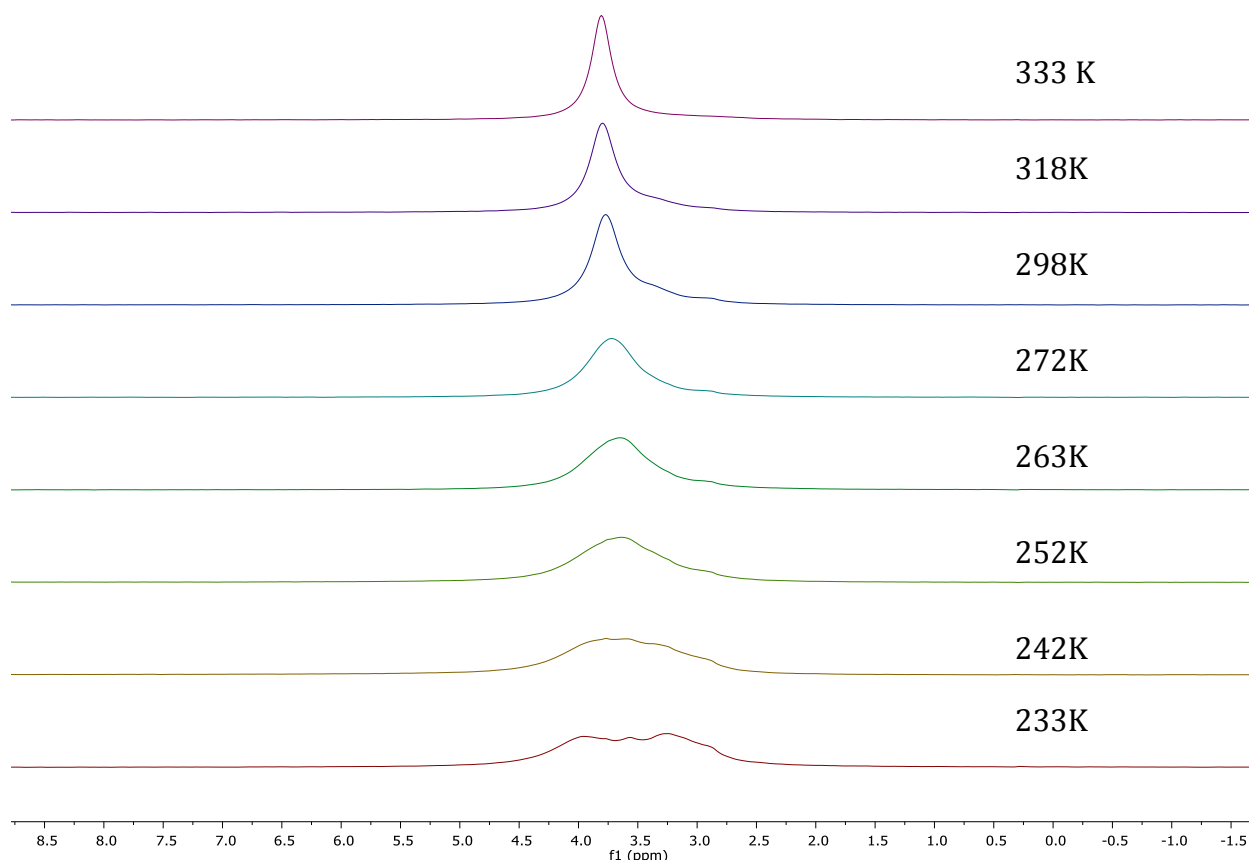


Figure 5. VT ⁷Li NMR spectrum (300 MHz, C₅D₅N) of **1** ($\omega_{1/2}$ values were calculated from the line fitting program in MestReNova NMR processing software).

For complex **4**, the spectra in C₆D₆ solutions showed broad peaks indicative of fluxional behavior (Figure S5) and this led us to pursue VT experiments in C₅D₅N as shown in Figure 6. The methylene groups of the homopiperazine and those between the nitrogen and the aromatic ring twist and are averaged at high temperatures but at low temperatures (233 and 253 K) the spectrum consists of separate peaks. Therefore, low temperature NMR data are reported for **4**

(Figure S6a). At room and high temperature, the separate peaks coalesce to yield single broad peaks as shown in Figure S6b.

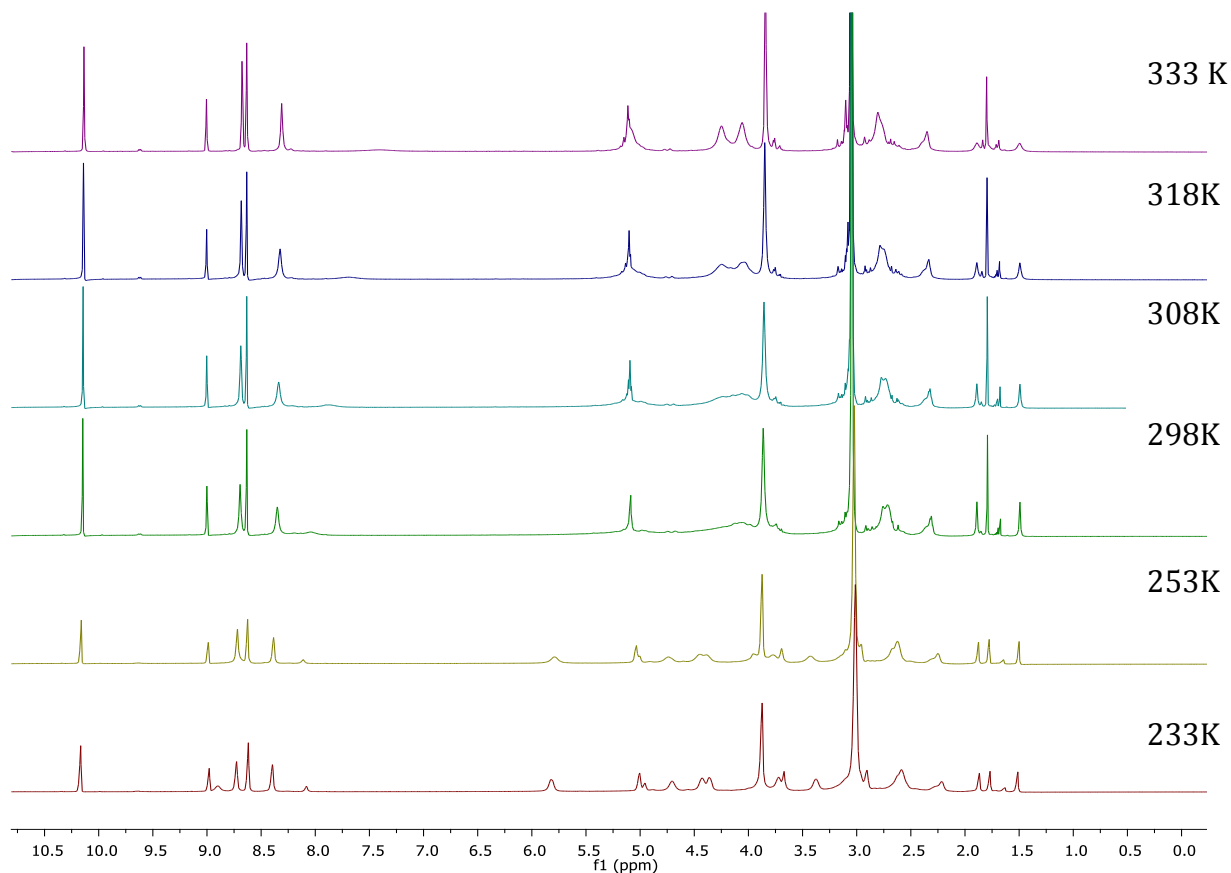


Figure 6. VT ¹H NMR spectrum (500 MHz, C₅D₅N) of **4**.

Pulse-gradient spin-echo (PGSE) NMR spectroscopy is a useful way to determine the size of molecules in solution.⁶⁸ As polymerization reactions were performed in dichloromethane, the nuclearity of **1** in CD₂Cl₂ was assessed by PGSE NMR spectroscopy. The value of the hydrodynamic radius ($r_{H,PGSE}$) of **1** was calculated using a previously described method and found to be 15.1 Å.³⁶ This is moderately smaller than $r_{X-ray} = 18.76$ Å, which was calculated according to $r_{X-ray} = (a^2 b)^{1/3}$ where a and b are the major and minor semi-axes of the prolate ellipsoid formed by the complex, as determined from the solid-state structure ($a = 19.94$ Å, $b = 16.61$ Å). This indicates that **1** likely retains its tetrametallic structure in this non-coordinating

solvent. However, it should be noted that this data reflects the solution-state structure at room temperature and bimetallic species may exist at elevated temperatures. Although many previously reported Li_4 phenolate complexes disaggregate in solution, the Kerton group have recently published a closely related Li_4 complex that also retains its aggregated state at room temperature in solution.⁶⁹

Polymerization of *rac*-lactide

The catalytic behavior of **1**, **2**, **3** and **4** in the ring-opening polymerization of *rac*-lactide in the presence and absence of benzyl alcohol as co-initiator was investigated.

Solvent free polymerization

In order to reduce reaction times and achieve higher turnover frequencies,^{4,70} polymerization reactions were conducted under bulk/melt conditions at high temperatures. The results are summarized in Table 1. ROP reactions were performed with **1**, **2**, **3** and **4** at 150 °C and no significant differences in reactivity were observed (entries 1-4). All complexes were stable and capable of initiating the ROP of *rac*-lactide, with or without co-initiator (benzyl alcohol, BnOH). Moreover, compared to work done previously with main group metals under the same conditions but with higher monomer loadings (greater than 50), higher conversions could be achieved in shorter reaction times with lower dispersities values using these complexes.⁷¹⁻⁷³ To study the effect of the temperature and the co-initiator, compound **3** was further scrutinized (entries 9-12). The complex was able to efficiently polymerize *rac*-lactide at 130 °C, which is particularly relevant to industry.⁴ For bulk polymerization, studies indicate a pseudo first-order dependence on the monomer concentration as shown in conversion vs. time plots (Figure S7). However, kinetic data cannot be obtained from such graphs because the reaction proceeds too quickly to ascertain initial rates where *rac*-lactide concentrations will still be high. In addition, as expected it was found that the conversion rates were greater with BnOH than its absence (entry 11 vs 9). The control of macromolecular features is also much improved when BnOH is used, both in terms of PDIs and agreement between M_{ncal} vs. M_n . All the generated polymers have molecular weights higher than the theoretical values (M_{ncal}), which might be attributed to inter- or intratransesterification reactions.⁷⁴⁻⁷⁵ Notably, the obtained dispersities (with or without

BnOH) were more narrow than previously reported values⁷¹⁻⁷³ for polymers prepared in the melt-phase suggesting a more controlled polymerization. It should be noted that the M_n values increase moderately with longer reaction times (entry 12 and 11). In addition, there was no significant difference in the molecular weights between the polymers produced at 150 °C and 130 °C. However, lower molecular weights were observed when polymerizations were run with higher monomer loadings (entry 13 and 14).

Table 1. Polymerization of *rac*-lactide using **1**, **2**, **3** and **4** in the presence and absence of BnOH in the melt phase

Entry	Complex	[LA] ₀ /[M] ₀ /[BnOH] ₀	t/min	T /°C	Conv /% ^[a]	$M_{\text{ncal}}^{\text{[b]}} \times 10^3$	$M_n^{\text{[c]}} \times 10^3$	$M_w/M_n^{\text{[c]}}$
1	1	50/1/0	90	150	98	7.1	13.0	1.30
2	2	50/1/0	90	150	97	7.0	10.2	1.10
3	3	50/1/0	90	150	99	7.1	12.0	1.14
4	4	50/1/0	90	150	96	7.0	11.3	1.20
5	1	50/1/1	90	150	98	7.1	8.2	1.05
6	2	50/1/1	90	150	98	7.2	9.2	1.06
7	3	50/1/1	90	150	99	7.2	9.0	1.20
8	4	50/1/0	90	150	99	7.2	10.3	1.10
9	3	50/1/0	10	130	93	6.7	14.0	1.14
10	3	50/1/0	120	130	98	7.0	16.2	1.21
11	3	50/1/1	5	130	97	7.1	9.4	1.04
12	3	50/1/1	120	130	99	7.2	11.0	1.18
13	2	250/1/0	90	150	73	26.3	8.0	1.22
14	2	250/1/1	90	150	99	35.8	6.4	1.18

[a] Determined by ¹H NMR spectroscopy. [b] The M_{ncal} value of the polymer was calculated with $M_{\text{ncal}} = ([\text{LA}]_0/[\text{M}]_0) \times 144.13 \times \text{conv. \%}/[\text{BnOH}] + 108.14$. [c] M_n (g mol⁻¹) determined by triple detection gel permeation chromatography (GPC) in THF using a dn/dc value of 0.049 mL g⁻¹.

Polymerizations in solution

1-4 were examined for ROP of *rac*-lactide in CH₂Cl₂ at room temperature. To examine solvent effects that may influence activities in these reactions, polymerization with **3** was further explored in THF and toluene. Representative results are reported in Table 2. All polymerizations

showed a first-order dependence on lactide concentration in the form of a linear relationship of $\ln([LA]_0/[LA]_t)$ versus time as shown in Figures 7-12 and S8-S12. The catalytic activities are highly influenced by the nature of the solvent and the presence of BnOH (initiator). For instance, performing the reaction in CH_2Cl_2 (entry 12) in the absence of BnOH using **3** resulted in a much faster reaction compared to toluene and THF (entries 14 and 16) with high conversion after only 80 min. However, the volume of solvent used in CH_2Cl_2 reactions was much smaller and therefore concentration will also have played a role. A large amount of toluene was essential due to the low solubility of LA in toluene at room temperature. Although concentration studies using **3** in CH_2Cl_2 were not performed, for **2** under similar conditions (entries 7 and 9), similar reaction rates were seen for both high and low monomer concentrations but polymers with significantly lower M_n values were obtained under more dilute reaction conditions. Compared to CH_2Cl_2 and toluene, lower conversions were observed when THF was employed and this could be due to the coordinating nature of THF, which competes with the incoming monomer for coordination at the metal center (entry 16 vs 12 and 14).^{28, 37, 72} Moreover, BnOH is able to significantly speed up the polymerizations carried out in THF (entry 17), whereas little difference in activities were observed for both CH_2Cl_2 and toluene (entries 13 and 15). Therefore, kinetic data for reactions performed in THF in the presence of BnOH could not be accurately obtained, as assumptions regarding the steady-state concentration of *rac*-lactide could not be made (Figure S8). It should be noted that with **3** low molecular weight oligomers were likely obtained when toluene and THF were used (entries 14-17) because no polymer precipitated upon the addition of cold methanol to reaction mixtures and therefore, GPC data were not obtained for these samples. The formation of low molecular weight species was confirmed by end group analysis where the 1H NMR spectra of the polymers. Integration of the $-OH$ end group resonance relative to the CH_3 group afforded low molecular weights polymers ($n = 5, 384$ g/mol).

Table 2. Polymerization of *rac*-lactide using **1**, **2**, **3** and **4** in the presence and absence of BnOH

Entry	Complex	[LA] ₀ /[M] ₀ /[BnOH] ₀	t/min	Conv /% ^[d]	$M_{\text{ncal}}^{[e]} \times 10^3$	$M_n^{[f]} \times 10^3$	$M_w/M_n^{[f]}$
1	1	250/1/0 ^[a]	80	92	33.1	28.0	1.31
2	1	250/1/1 ^[a]	80	93	33.6	17.2	1.29
3	1	250/1/2 ^[a]	40	92	16.7	8.00	1.15
4	1	250/1/2 ^[a]	300	99	17.9	12.1	1.24
5	1	250/1/4 ^[a]	30	90	8.2	4.00	1.19
6	1	250/1/4 ^[a]	300	95	8.7	7.80	1.15
7	2^k	250/1/0 ^[a]	40	73	26.3	24.0	1.30
8	2^k	250/1/1 ^[a]	7	93	33.6	19.0	1.18
9 ^h	2^k	250/1/0 ^[a]	60	53	19.1	13.0	1.11
10	2^k	250/1/0 ^[c]	180	55	19.8	21.0	1.10
11	3^k	50/1/0 ^[a]	5	100	7.2	ND	–
12	3^k	250/1/0 ^[a]	80	94	33.9	33.4	1.33
13	3^k	250/1/1 ^[a]	80	91	33.0	29.6	1.32
14	3^k	250/1/0 ^[b]	180	69	24.9	ND ^[g]	-
15	3^k	250/1/1 ^[b]	120	93	33.6	ND ^[g]	-
16	3^k	250/1/0 ^[c]	240	52	18.7	ND ^[g]	-
17	3^k	250/1/1 ^[c]	3	98	35.4	ND ^[g]	-
18	4	250/1/0 ^[a]	40	91	32.8	26.3	1.20
19	4	250/1/1 ^[a]	5	94	34.1	22.4	1.36
20	4	250/1/1 ^[a]	300	99	35.8	34.8	1.22
21	4	250/1/0 ^[c]	3	90	32.4	36.2	1.41
22	4	250/1/1 ^[c]	3	100	36.1	20.2	1.10
23 ⁱ	n-BuLi	250/1/1 ^[a]	60	96	34.7	11.8	1.13
24 ^j	NaH	250/1/1 ^[a]	>540	65	23.5	11.7	1.47

All reactions performed at 25 °C [a] CH₂Cl₂ (5 mL). [b] Toluene (30 mL). [c] THF (20 mL). [d] Determined by ¹H NMR spectroscopy. [e] The M_{ncal} value of the polymer was calculated with $M_{\text{ncal}} = ([\text{LA}]_0/[\text{M}]_0) \times 144.13 \times \text{conv. \%}/[\text{BnOH}] + 108.14$. [f] The M_n (g mol⁻¹) determined by triple detection gel permeation chromatography (GPC) in THF using a dn/dc value of 0.049 mL g⁻¹. [g] Low molecular weight oligomers formed. Data from NMR end group analysis: n = 5, $M_n \sim 384$ g mol⁻¹. [h] CH₂Cl₂ (20 mL). [i] 0.2 mL *n*-BuLi (0.16 M, 0.02 mmol) was added to CH₂Cl₂ solution (5 mL) containing *rac*-lactide (2.95 mmol) and BnOH (0.0118) at 25 °C. [j] NaH (0.16 M, 0.047 mmol) was added to CH₂Cl₂ solution (5 mL) containing *rac*-lactide (2.95 mmol) and BnOH (0.0118 mmol) at 25 °C. [k] P_r values for polymers produced by **2** and **3** were typically 0.44-0.47.

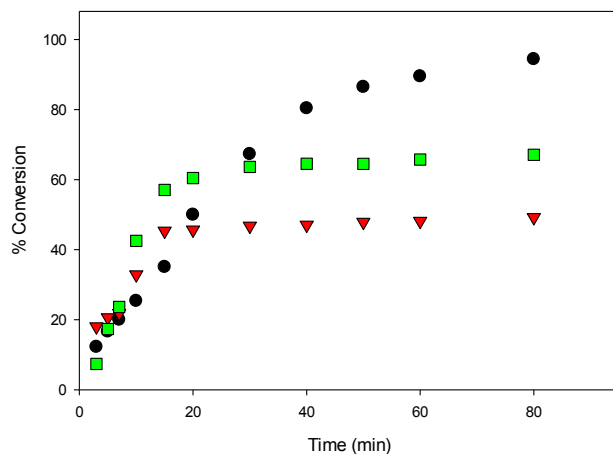


Figure 7. Conversion (%) vs. time for the ROP of LA initiated by **3** under the conditions in Table 2, entries 12, 14 and 16. ● CH₂Cl₂, ■ Toluene, ▼ THF.

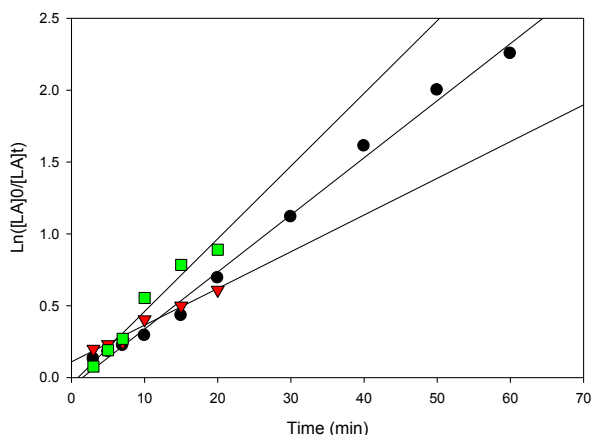


Figure 8. First-order plot of LA consumption initiated by **3** according to the conditions in Table 2, entries 12, 14 and 16. ● CH₂Cl₂ ($y = 0.0397x - 0.0594$, $R^2 = 0.9933$), ■ Toluene ($0.0506x - 0.0448$, $R^2 = 0.96$), ▼ THF ($y = 0.0255x + 0.1097$, $R^2 = 0.9742$).

The steric bulk of substituents on the aromatic rings was found to have less influence on the activity compared to the identity of the metal center (entry 1 vs 12). That is, the activity trend decreases in the order $4 > 2 > 3 \geq 1$ and can be partially explained by the larger ionic radius of sodium compared to lithium.^{26, 38, 47-48} It is not surprising that the initiator is not required for ROP catalyzed by **1** and **3** as the same observation was reported by Kozak's group for related amine-

bis(phenolate) lithium complexes.³⁵ In contrast, the presence of the initiator was necessary to accelerate reactions using sodium complexes (entry 18 vs 19) and this has also been reported by others.⁴⁹⁻⁵⁰ The observed M_n values of these solution-phase polymers are in some cases close to the expected molecular weights and the low dispersities obtained (ranging from 1.10-1.36) indicated that the polymerization has characteristics of controlled propagation. The controlled behavior is also demonstrated by the linear relationship between M_n and % conversion, and the narrow dispersity of the polymers throughout their chain growth (Figure 11).^{30, 36, 75}

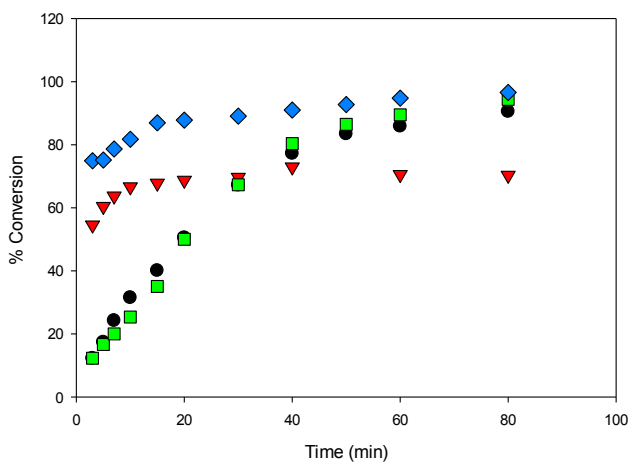


Figure 9. Conversion (%) vs. time for the ROP of LA initiated by **1**, **2**, **3** and **4** in CH_2Cl_2 under the conditions in Table 2, entries 1, 7, 12 and 18. ● **1**, ▼ **2**, ■ **3**, ◆ **4**.

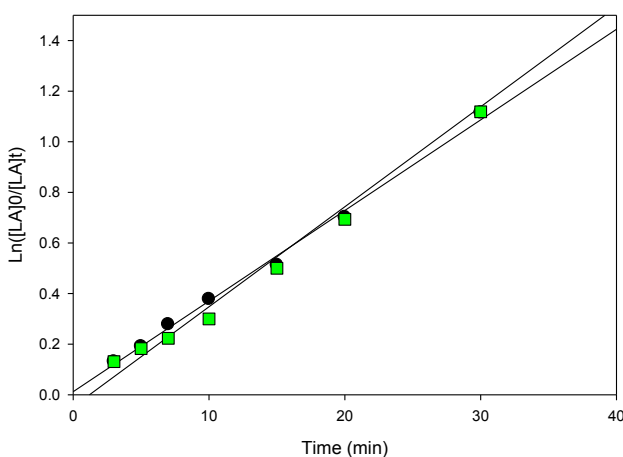


Figure 10. First-order plot of LA consumption initiated by **1** and **3** in CH_2Cl_2 under the conditions in Table 2, entries 1 and 12. ● **1** ($y = 0.0358x + 0.0123$, $R^2 = 0.9954$), ■ **3** ($y = 0.0395x - 0.0471$, $R^2 = 0.9951$).

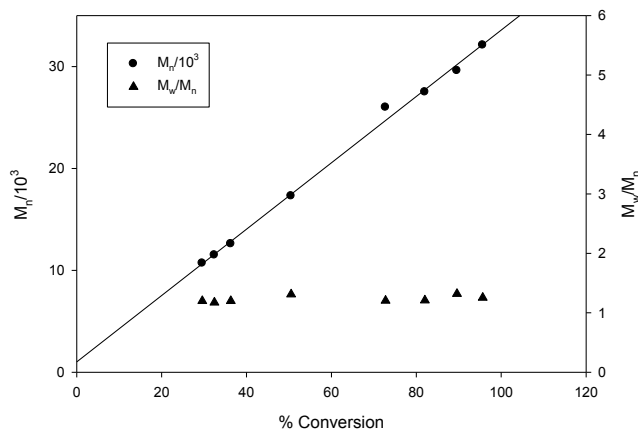


Figure 11. Plot of PLA M_n and dispersity (M_w/M_n) as a function of *rac*-lactide conversion under the conditions in Table 2, entry 13.

Increasing the amount of BnOH can be used to control both the molecular weight and the polymerization rate. For instance, upon doubling the amount of alcohol to two equiv. per lithium center, the molecular weight of the polymer diminished to half its original value. While it decreased to one quarter with the addition of four equiv. BnOH (entries 3 and 5). In addition, as shown in Figures 12 and S12, in both cases the reaction rates are faster compared to performing the reaction with one equiv. of benzyl alcohol. Such observations are an important feature of well-behaved *immortal* ROP with reversible and fast chain transfer between dormant and growing macroalcohols.^{36, 75} Performing the reaction at longer times gives higher molecular weight compared with short reaction times (*e.g.* entry 3 vs 4) suggesting the occurrence of chain transfer reactions during polymerization.³⁶

Moreover, a comparison of the catalytic activities of **1-4** and related ligand-free systems has been performed under identical ROP conditions. One equiv. of *n*-BuLi or four equiv. NaH was added into a CH₂Cl₂ solution containing 250 equiv. of *rac*-lactide and one equiv. of BnOH (entries 23 and 24). ROP of lactide using the *in situ* formed lithium alkoxide was complete within 60 min with a conversion of 96% whereas the sodium alkoxide exhibited lower efficiency with moderate conversion (65%) and a more disperse polymer was produced. All the generated polymers from ligand-free systems had lower molecular weights than those produced with **1-4**.

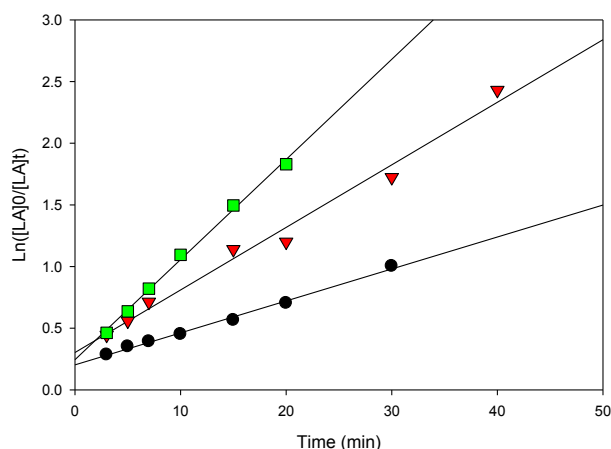


Figure 12. First-order plot of LA consumption initiated by **1** in CH_2Cl_2 under the conditions in Table 2, entries 2, 3 and 5. ● 1 eq. BnOH ($y = 0.0507x + 0.3033$, $R^2 = 0.9858$), ▼ 2 eq. BnOH ($y = 0.0259x + 0.2026$, $R^2 = 0.9944$), ■ 4 eq. BnOH ($y = 0.0812x + 0.2446$, $R^2 = 0.9963$).

NMR spectroscopy of polymers in bulk and solvent polymerization

Similar signals were found in ^1H NMR spectra for the polymers from reactions performed in both the absence and the presence of one equiv. BnOH: a hydroxyl group (d) at 2.72 ppm, a hydroxymethine group (HOCH-) (c) at 4.35 ppm, methyl groups (CH-CH_3) (a) between 1.50 and 1.55 ppm (Figure S13).³⁵ No evidence for benzyl ester group formation could be found when one equiv. BnOH was added, suggesting the presence of inter or intratransesterification reactions. However, a benzyl ester group (OCH_2Ph) (e) at 7.32 ppm, hydroxyl group (f) and hydroxymethine group (HOCH-) (c) at 4.33 ppm were observed as end-groups with the addition of two and four equiv. BnOH (Figure S14).

Determination of the polymer tacticity was achieved by homodecoupled ^1H and ^{13}C NMR experiments (Figure S15 and S16, respectively). The probability of racemic enchainment (probability of forming a new racemic diad) was calculated from the deconvoluted homonuclear decoupled ^1H NMR spectra.⁷ The P_r values for polymers produced by **2** and **3** are within the range 0.44-0.47, which indicates a negligible isotactic bias (a value of 0.5 is expected for a perfectly atactic polymer).⁵⁰ Isotactic polymers have previously been reported in some cases for lithium and sodium phenolates.^{35, 50} In ^{13}C spectra the signal assignments in the methine region show multiple possible tetrad sequences *iii*, *iis*, *sii* and *isi* which is in good agreement with previously reported ROP of *rac*-lactide by an achiral catalyst.⁷⁶ However, the unusual increase in

the intensity of the iss, sss and ssi tetrads in Figure S15 and the presence of weaker peaks at 69.58, 69.47 and 69.25 ppm in Figure S16 indicate stereorandom transesterification during the course of the polymerization reactions.^{35, 50, 77}

Mass spectrometry of polymers

MALDI-TOF analysis of PLA was conducted with 2,5-dihydroxybenzoic acid (DHBA) as the matrix with a ratio of 5:1 (matrix:PLA). Using reflectron mode, the peaks are separated by 72 mass units and three major repeating masses were observed in the case of polymers obtained in the absence of BnOH and 1 equiv. BnOH. As shown in Figure 13, two intense peaks (B and C, $n = 12$, $m/z = 919$ and 935) were assigned as $\text{CH}_3\text{O}[\text{C}=\text{O})\text{CHMeO}]_n\text{H.Na}^+$ and $\text{CH}_3\text{O}[\text{C}=\text{O})\text{CHMeO}]_n\text{H.K}^+$. In addition, a less intense series of peaks for cyclic polymer (A, $n = 12$, $m/z = 903$) clustered with a Na^+ ion were seen, pointing to the presence of intrachain transesterification side reactions. The termination with methoxy groups probably stems from initiation of polymerization by nucleophilic attack of the phenolate oxygen on the carbonyl followed by quenching with methanol. Similar end-groups have been observed by others recently.⁷⁸ The polymers formed with 2 and 4 equiv. BnOH show only one major repeating series (A, $n = 12$, $m/z = 919$) that corresponds to polymers capped with methoxy groups $\text{CH}_3\text{O}[\text{C}=\text{O})\text{CHMeO}]_n\text{H.Na}^+$ without any evidence for cyclic formation or the benzyl ester groups (Figure 14). This contrasts with the NMR data obtained, which showed the presence of the expected benzyl ester groups.

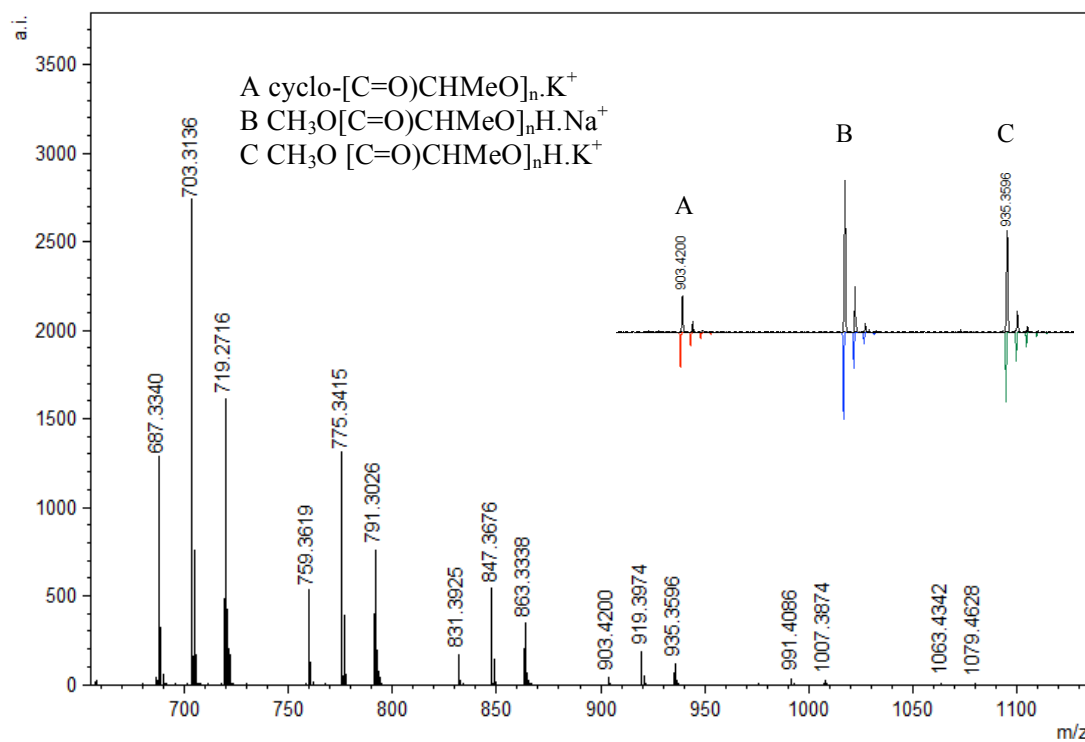


Figure 13. Representative region of the MALDI-TOF mass spectrum (reflectron mode) of PLA under the conditions in Table 1, entry 12 (similar spectra obtained for PLA from entries 13, 18 and 19).

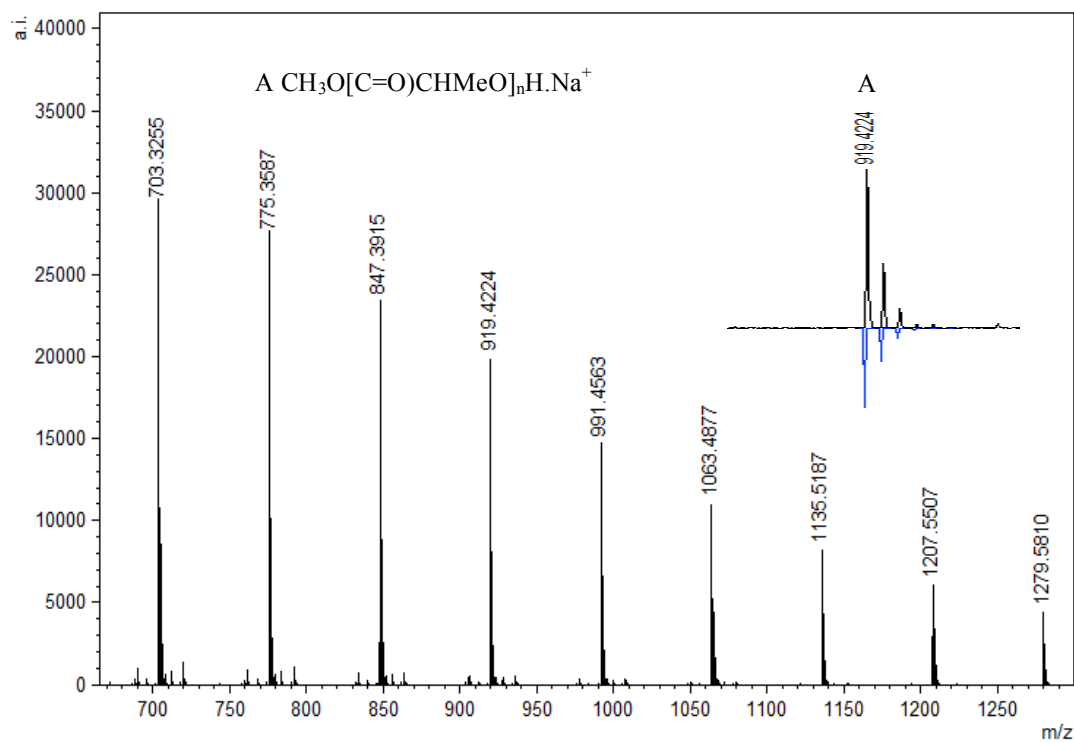


Figure 14. Representative region of the MALDI-TOF mass spectrum (reflectron mode) of PLA under the conditions in Table 1, entry 3 (similar spectrum obtained for PLA from entry 5).

Mechanistic proposal

In the absence of BnOH, the initiation step of ROP of *rac*-lactide could be proceeding via coordination insertion of the monomer into the metal-phenoxide bond as shown in Figure 15.^{35, 37, 46, 79-83} Comparison of ⁷Li NMR spectra recorded in the absence and presence of *rac*-lactide strongly suggests the formation of an additional Li species upon addition of a small amount of *rac*-lactide with the growth of a new peak at 1.30 ppm (Figure S17). This supports the coordination step of the mechanisms described herein. To investigate the ROP reaction in the presence of BnOH, stoichiometric reactions with **1** in CD₂Cl₂ at room temperature were monitored by ¹H NMR spectroscopy. The spectra of a 1:1 (per 2 metal centers) reaction of **1** and BnOH confirms the formation of both {N₂O₂^{BuBuPip}}H (11.05 ppm) and BnO-Li, the latter appearing as overlapping peaks around 7.34 ppm (Figure S18, 19 and 20). Addition of 1 equiv. of *rac*-lactide yields benzyl-2-((2-hydroxypropanoyl)oxy)propanoate, the product of lactide ring-opening. Unfortunately, we were unable to isolate this species. In spite of this, we propose that ring-opening polymerization is occurring through a coordination–insertion mechanism, where benzyl alcohol is sufficiently activated by the lithium centers and protonates the phenolate group to yield a new lithium complex, followed by attack of the benzyl alkoxide group at the carbonyl group of *rac*-lactide (Figure 16).^{35, 37, 46, 79-83} We also note that the reactivity of BnOLi formed *in situ* affords similar polymerization data. From DOSY NMR experiments above, the predominant Li species present in CD₂Cl₂ (in the absence of lactide and BnOH) is the tetralithium complex. Therefore, it is likely that the alcohol also plays a role in assisting the dissociation process in solution, as we assume this will occur under reaction conditions to allow space for the growing polymer chain.

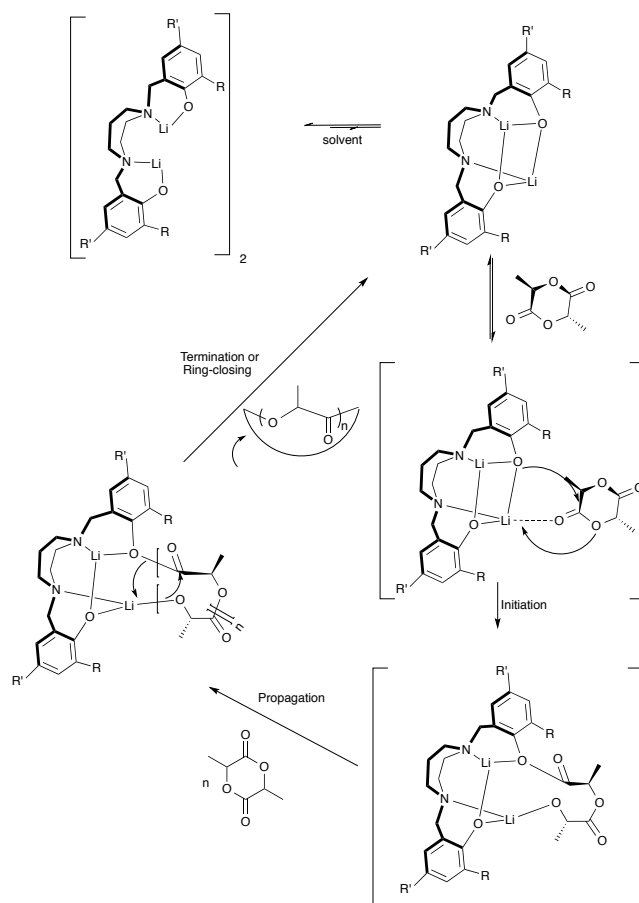


Figure 15. Proposed mechanism of the ROP of *rac*-LA in the absence of BnOH initiated by lithium and sodium amine-bis(phenolate) complexes (THF omitted for clarity, coordination sphere of the metals will be completed by either LA or THF).

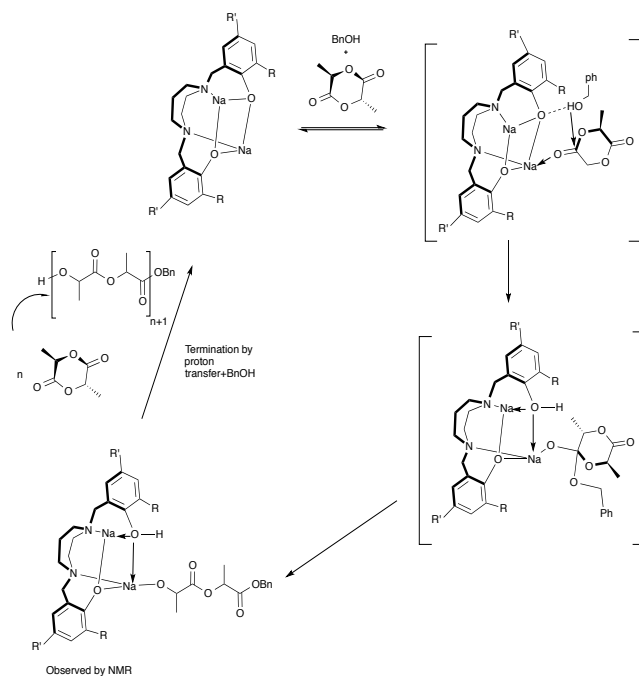


Figure 16. Proposed mechanism of the ROP of *rac*-LA in the presence of BnOH initiated by sodium amine bis(phenolate) complexes (THF omitted for clarity, coordination sphere of the metals will be completed by either LA or THF).

Experimental

General experimental conditions

All operations were carried out under an atmosphere of dry, oxygen-free nitrogen using standard Schlenk techniques or an MBraun Labmaster DP glove box. Anhydrous THF, benzene were distilled from sodium benzophenone ketyl under nitrogen. Toluene and pentane were purified by an MBraun Manual Solvent Purification System. Reagents were purchased either from Aldrich or Alfa Aesar and used without further purification. *Rac*-lactide were purchased from Alfa Aesar and dried over Na₂SO₄ in THF, recrystallized and stored under nitrogen in ampules. Benzyl alcohol was purchased from Alfa Aesar and dried over activated 4 Å molecular sieves, distilled under reduced pressure and stored under nitrogen in an ampule prior to use. Deuterated solvents were purchased from Cambridge Isotope Laboratories and purified and degassed through freeze-vacuum-thaw cycles and stored under nitrogen in ampules fitted with Teflon valves. NaH was washed twice with hexane, as it was purchased as a suspension in mineral oil. Aqueous formaldehyde (37 wt%) was purchased from Fisher Scientific and also used without further purification.

Instrumentation

¹H, ¹³C and ¹H{¹H} NMR spectra were recorded on a Bruker Avance 500 or 300 MHz spectrometer at 25 °C (unless otherwise stated) and were referenced internally using the residual proton and ¹³C resonances of the solvent. ⁷Li NMR was recorded on a Bruker 300 MHz spectrometer and referenced externally to LiCl in D₂O. MALDI-TOF MS spectra were performed using Applied Biosystems 4800 MALDI TOF/TOF Analyzer equipped with a reflectron, delayed ion extraction and high performance nitrogen laser (200 Hz operating at 355 nm). Samples were prepared in the glove box and sealed under nitrogen in a Ziploc[®] bag for transport to the instrument at a concentration of 10.0 mg/mL in toluene. For ligands and complexes, anthracene was used as the matrix, which was mixed at a concentration of 10.0 mg/mL. For the polymers, mass spectra were recorded in reflectron mode and 2-(4-hydroxyphenylazo)benzoic acid (HABA) was used as the matrix and purified tetrahydrofuran was used as the solvent for depositing analytes onto the instrument's plate. The matrix was dissolved in THF at a concentration of 10 mg mL⁻¹. Polymer was dissolved in THF at approximately 1 mg

mL⁻¹. The matrix and polymer solutions were mixed together at a ratio of 5 to 1; 1 μ L of this was spotted on the MALDI plate and left to dry. Images of mass spectra were prepared using mMassTM software (www.mmass.org). GPC analysis was performed in THF at 25 °C on a Wyatt Triple Detection (triple angle light scattering, viscometry and refractive index) system with a Agilent 2600 series LC for sample and solvent handling, and two Phenogel 10³ Å 300 × 4.60 mm columns. Samples were dissolved in THF at a concentration of 1 mg mL⁻¹, left to equilibrate for ~2 h and passed through syringe filters before analysis. An eluent flow rate of 0.30 mL/min and 100 μ L injection volume were used. Molecular weights (g mol⁻¹) were determined by triple detection using a dn/dc value of 0.049 mL g⁻¹. Conversions were determined by integration of the methyl signals due to the residual *rac*-lactide and produced poly-(*rac*-lactide). Elemental analyses were performed by Canadian Microanalytical Service Ltd., Delta, B.C. Canada.

Diffusion NMR measurements were performed on a Bruker Avance 500 NMR spectrometer equipped with a 5 mm TXI probe and a z-gradient coil with a maximum strength of 5.35 G cm⁻¹ at 298 K. The sample was run in CD₂Cl₂ at a concentration of 10.0 mM. The 90° pulse length and the relaxation time T_1 of the sample were determined before running the DOSY experiment. A standard 2D sequence with double stimulated echo and spoil gradient (DSTEBPGP3s) was used. The relaxation delay was set at 10 s. The gradient strength was calibrated by using the self-diffusion coefficient of residual HOD in D₂O (1.9×10^{-9} m² s⁻¹). For each experiment, the gradient strength was increased from 2 – 95% in 32 equally spaced steps with 16 scans per increment. Values of δ (gradient pulse length) and Δ (diffusion time) were optimized on the sample to give an intensity of between 5 and 10% of the initial intensity at 95% gradient strength and were set to 1 ms and 100 ms respectively. The solvent peak was used as an internal standard to measure the viscosity of each sample, $D_0(\text{CD}_2\text{Cl}_2) = 3.28 \times 10^{-9}$ m² s⁻¹ and $\eta_0 = 0.413$ cp at 298 K.⁸⁴ The data were plotted using DynamicCenter (Bruker) and the diffusion coefficient (D) was extracted by fitting a mono exponential function ($\ln(I/I^0) = -\gamma^2 \delta^2 G^2 (\Delta - \delta/3) D t$) with the data analysis component of the software. The hydrodynamic radius of the complex ($r_{H,PGSE}$) was calculated using the procedure outlined by Carpentier, Sarazin and co-workers.³⁶ An average of the values of D_t (9.86×10^{-10} m² s⁻¹ \pm 0.65) found for 3 separate peaks in the ¹H PGSE NMR spectrum was used in the calculations. $r_H(\text{CD}_2\text{Cl}_2) = 2.49$ Å was used.⁸⁵

Synthesis and Characterization

Synthesis of $\text{H}_2[\text{N}_2\text{O}_2^{\text{BuBuPip}}]$ A mixture of 2,4-di-*tert*-butylphenol (24.4 g, 0.123 mol), 37% w/w formaldehyde (10.0 mL, 123 mmol) and homopiperazine (6.22 g, 0.0615 mol) in water (100 ml) was stirred and heated to reflux for 24 hours. Upon cooling to room temperature, solvents were decanted from the resulting white solid, which was recrystallized from methanol and chloroform to afford a pure white powder (32.4 g, 98%). Anal. calc'd for $\text{C}_{35}\text{H}_{56}\text{N}_2\text{O}_2$: C, 78.31; H, 10.51; N, 5.22. Found: C, 78.19; H, 10.33; N, 5.11. ^1H NMR (300 MHz, 298 K, CDCl_3) δ 1.25 (18H, s, ArC-C(CH_3)₃), 1.40 (18H, s, ArC-C(CH_3)₃), 1.89 (2H, quintet, $^3J_{\text{HH}} = 6.04$ Hz, N- $\text{CH}_2\{\text{CH}_2\}\text{CH}_2\text{-N}$), 2.75 (4H, s, N- $\text{CH}_2\{\text{CH}_2\}\text{CH}_2\text{-N}$), 2.80 (4H, t, $^3J_{\text{HH}} = 6$ Hz, N- $\text{CH}_2\text{CH}_2\text{-N}$), 3.75 (4H, s, ArC- $\text{CH}_2\text{-N}$), 6.79 (2H, d, $^2J_{\text{HH}} = 2.3$ Hz, ArH), 7.19 (2H, d, $^2J_{\text{HH}} = 2.3$, ArH), 11.03 (2H, s, OH). ^{13}C $\{^1\text{H}\}$ NMR (300 MHz, 298 K, C_6D_6) δ 27.2 (N- $\text{CH}_2\{\text{CH}_2\}\text{CH}_2\text{-N}$), 30.4 (ArC-C-(CH_3)₃), 32.4 (ArC-C-(CH_3)₃), 34.7 (ArC-C-(CH_3)₃), 35.7 (ArC-C-(CH_3)₃), 53.2 (N- $\text{CH}_2\text{CH}_2\text{-N}$), 54.9 (N- $\text{CH}_2\{\text{CH}_2\}\text{CH}_2\text{-N}$), 63.1 (ArC- $\text{CH}_2\text{-N}$), 122.1 (ArC- $\text{CH}_2\text{-N}$), 123.6 (ArCH), 124.0 (ArCH), 136.5 (ArC-C(CH_3)₃), 141.1 (ArC-C(CH_3)₃), 155.6 (ArC-O). MS (MALDI-TOF) m/z (% ion): 536.32 (100, $\text{H}_2[\text{N}_2\text{O}_2^{\text{BuBuPip}}]^{++}$).

Synthesis of $\text{H}_2[\text{N}_2\text{O}_2^{\text{BuMePip}}]$ This was prepared in a similar manner to $\text{H}_2[\text{N}_2\text{O}_2^{\text{BuBuPip}}]$ to yield a pure white powder (26.1 g, 93.6%). Anal. calc'd for $\text{C}_{29}\text{H}_{44}\text{N}_2\text{O}_2$: C, 76.95; H, 9.80; N, 6.19. Found: C, 77.11; H, 9.87; N, 6.12. ^1H NMR (300 MHz, 298 K, CDCl_3) δ 1.43 (18H, s, ArC-C(CH_3)₃), 1.89 (2H, quintet, $^3J_{\text{HH}} = 6.01$ Hz, N- $\text{CH}_2\{\text{CH}_2\}\text{CH}_2\text{-N}$), 2.25 (6H, s, ArC- CH_3), 2.77 (4H, s, N- $\text{CH}_2\{\text{CH}_2\}\text{CH}_2\text{-N}$), 2.82 (4H, t, $^3J_{\text{HH}} = 6.1$ Hz, N- $\text{CH}_2\text{CH}_2\text{-N}$), 3.75 (4H, s, ArC- $\text{CH}_2\text{-N}$), 6.66 (2H, s, ArH), 7.01 (2H, s, ArH), 11.0 (2H, s, OH). ^{13}C $\{^1\text{H}\}$ NMR (300 MHz, 298 K, CDCl_3) δ 21.0 (ArC- CH_3), 27.0 (N- $\text{CH}_2\{\text{CH}_2\}\text{CH}_2\text{-N}$), 29.7 (ArC-C-(CH_3)₃), 34.8 (ArC-C-(CH_3)₃), 53.2 (N- $\text{CH}_2\text{CH}_2\text{-N}$), 54.6 (N- $\text{CH}_2\{\text{CH}_2\}\text{CH}_2\text{-N}$), 62.2 (ArC- $\text{CH}_2\text{-N}$), 122.1 (ArC- $\text{CH}_2\text{-N}$), 127.0 (ArCH), 127.4 (ArCH), 127.5 (ArC- CH_3), 136.6 (ArC-C-(CH_3)₃), 154.6 (ArC-O). MS (MALDI-TOF) m/z (% ion): 452.31(100, $\text{H}_2[\text{N}_2\text{O}_2^{\text{BuMePip}}]^{++}$).

Synthesis of **1** $\text{H}_2[\text{O}_2\text{N}_2]^{\text{BuBuPip}}$ (2.01 g, 3.7 mmol) was dissolved in THF (50 mL) and cooled to -78 °C. *n*-Butyllithium (1.6 M, 5.0 ml, 8.14 mmol) was slowly added *via* cannula to afford a yellow solution, which was warmed to room temperature and stirred for 72 h. Solvent was removed under vacuum; the product was washed with cold pentane (10 mL). The product was then

filtered and dried under vacuum to yield (2.36 g, 97%) of a pale yellow product. Anal. calc'd for $C_{35}H_{54}Li_2N_2O_2(0.8 Li_2O \cdot 0.35 C_5H_{12})$: C, 73.83; H, 9.81; N, 4.69. Found: C, 73.74; H, 10.03; N, 4.91. 1H NMR (300 MHz, 298 K, C_6D_6) δ 1.19 (8H, s, CH_2 , THF), 1.47 (18H, s, $ArC-C(CH_3)_3$), 1.68 (18H, s, $ArC-C(CH_3)_3$), 1.89 (6H, br, $N-CH_2\{CH_2\}CH_2-N$), 2.71 (4H, s, $N-CH_2CH_2-N$), 3.38 (8H, s, CH_2 , THF), 3.58 (4H, s, $ArC-CH_2-N$), 7.05 (2H, d, $^2J_{HH} = 2.2$ Hz, ArH), 7.6 (2H, d, $^2J_{HH} = 2.2$ Hz, ArH). 1H NMR (500 MHz, 298 K, C_5D_5N) δ 1.42 (18H, s, $ArC-C(CH_3)_3$), 1.53 (18H, s, $ArC-C(CH_3)_3$), 1.63 (4H, m, CH_2 , $^3J_{HH} = 6.5$ Hz, THF), 1.68 (6H, s, $CH_2\{CH_2\}CH_2-N$), 2.77 (4H, br, $N-CH_2CH_2-N$), 3.7 (4H, m, CH_2 , $^3J_{HH} = 6.5$ Hz, THF), 3.86 (4H, s, $ArC-CH_2-N$), 7.18 (2H, s, ArH), 7.53 (2H, s, ArH). ^{13}C $\{^1H\}$ NMR (300 MHz, 298 K, $CDCl_3$) δ 27.0 (CH_2 , THF), 29.8 ($ArC-C-(CH_3)_3$), 31.9 ($ArC-C-(CH_3)_3$), 34.4 ($ArC-C-(CH_3)_3$), 35.1 ($ArC-C-(CH_3)_3$), 53.3 ($N-CH_2CH_2-N$), 54.7 ($N-CH_2\{CH_2\}CH_2-N$), 62.7 ($ArC-CH_2-N$), 100.2 ($ArC-CH_2-N$), 121.4 ($ArCH$), 123.6 ($ArCH$), 135.9 ($ArC-C(CH_3)_3$), 140.8 ($ArC-C(CH_3)_3$). ^{13}C $\{^1H\}$ NMR (300 MHz, 298 K, C_6D_6) δ 25.6 (CH_2 , THF), 27.4 ($N-CH_2\{CH_2\}CH_2-N$), 31.0 ($ArC-C-(CH_3)_3$), 32.8 ($ArC-C-(CH_3)_3$), 34.5 ($ArC-C-(CH_3)_3$), 35.7 ($ArC-C-(CH_3)_3$), 51.0 ($N-CH_2CH_2-N$), 53.4 ($N-CH_2\{CH_2\}CH_2-N$), 62.8 ($ArC-CH_2-N$), 68.5 (CH_2 , THF), 123.9 ($ArC-CH_2-N$), 126.1 ($ArCH$), 127.2 ($ArCH$), 134.0 ($ArC-C(CH_3)_3$), 136.9 ($ArC-C(CH_3)_3$), 164.2 ($ArC-O$). ^{13}C $\{^1H\}$ NMR (300 MHz, 298 K, C_5D_5N) δ 26.3 (CH_2 , THF), 27.4 ($N-CH_2\{CH_2\}CH_2-N$), 31.1 ($ArC-C-(CH_3)_3$), 32.8 ($ArC-C-(CH_3)_3$), 34.5 ($ArC-C-(CH_3)_3$), 35.9 ($ArC-C-(CH_3)_3$), 51.8 ($N-CH_2CH_2-N$), 53.9 ($N-CH_2\{CH_2\}CH_2-N$), 62.8 ($ArC-CH_2-N$), 68.3 (CH_2 , THF), 126.4 ($ArCH$), 127.5 ($ArCH$), 132.8 ($ArC-C(CH_3)_3$), 137.5 ($ArC-C(CH_3)_3$), 166.0 ($ArC-O$). 7Li $\{^1H\}$ NMR (C_6D_6 , 298 K, δ) 1.58. MS (MALDI-TOF) m/z (% ion): 548.4 (100, $Li_2[N_2O_2^{BuBuPip}]^{+}$).

Synthesis of 2 $H_2[O_2N_2]^{BuBuPip}$ (2.01 g, 3.7 mmol) was dissolved in THF (50 mL) and cooled to -78 °C. Sodium hydride (0.357 g, 14.8 mmol) was dissolved in THF (20 mL) and slowly added *via* cannula to afford a white suspension solution, which was warmed and stirred for 72 h. Solvent was removed under vacuum; the product was washed with cold pentane (10 mL). The product was then filtered and dried under vacuum to yield (2.36 g, 98%) of a deep yellow product. Anal. calc'd for $C_{35}H_{54}Na_2N_2O_2$: C, 72.38; H, 9.37; N, 4.82. Found: C, 66.11; H, 10.49; N, 3.84. 1H NMR (300 MHz, 298 K, C_6D_6) δ 1.28 (8H, m, $^3J_{HH} = 6.6$ Hz, CH_2 , THF), 1.29 (18H, s, $ArC-C(CH_3)_3$), 1.70 (18H, s, $ArC-C(CH_3)_3$), 1.90 (2H, br, $N-CH_2\{CH_2\}CH_2-N$), 2.47 (4H, br, $N-CH_2\{CH_2\}CH_2-N$), 2.81 (2H, br, $N-CH_2CH_2-N$), 3.03 (2H, br, $N-CH_2CH_2-N$), 3.25 (8H, m, $^3J_{HH} =$

6.6 Hz, CH_2 , THF), 4.02 (4H, br, ArC- CH_2 -N), 6.99 (2H, d, $^2J_{HH} = 2.3$ Hz, ArH), 7.51 (2H, d, $^2J_{HH} = 2.3$ Hz, ArH). ^{13}C { 1H } NMR (300 MHz, 298 K, C_5D_5N) δ 26.3 (CH_2 , THF), 27.9 (N- $CH_2\{CH_2\}CH_2$ -N), 31.2 (ArC-C-(CH_3) $_3$), 33.1 (ArC-C-(CH_3) $_3$), 34.5 (ArC-C-(CH_3) $_3$), 36.1 (ArC-C-(CH_3) $_3$), 54.2 (N- CH_2CH_2 -N), 56.7 (N- $CH_2\{CH_2\}CH_2$ -N), 64.7 (ArC- CH_2 -N), 68.3 (CH_2 , THF), 123.3 (ArC- CH_2 -N), 126.7 (ArCH), 127.1 (ArCH), 130.4 (ArC-C(CH_3) $_3$), 137.7 (ArC-C(CH_3) $_3$), 168.8 (ArC-O). ^{13}C { 1H } NMR (300 MHz, 298 K, $CDCl_3$) δ (ppm) 25.8 (CH_2 , THF), 27.0 (N- $CH_2\{CH_2\}CH_2$ -N), 29.8 (ArC-C-(CH_3) $_3$), 31.9 (ArC-C-(CH_3) $_3$), 34.4 (ArC-C-(CH_3) $_3$), 35.1 (ArC-C-(CH_3) $_3$), 53.3 (N- CH_2CH_2 -N), 54.7 (N- $CH_2\{CH_2\}CH_2$ -N), 62.7 (ArC- CH_2 -N), 68.2 (CH_2 , THF), 100.2 (ArC- CH_2 -N), 121.5 (ArCH), 123.7 (ArCH), 135.8 (ArC-C(CH_3) $_3$), 140.9 (ArC-C(CH_3) $_3$), 154.3 (ArC-O). MS (MALDI-TOF) m/z (% ion): 580.3 (100, $Na_2[N_2O_2^{BuBuPip}]^{+}$).

Synthesis of 3 This was prepared in a similar manner to **1** to yield (2.06 g, 97%) of a pale yellow product. Anal. calc'd for $C_{29}H_{42}Li_2N_2O_2$ (1.95 $Li_2O \cdot 1.2 C_5H_{12}$): C, 68.98; H, 9.33; N, 4.60. Found: C, 68.64; H, 9.73; N, 5.00. 1H NMR (300 MHz, 298 K, C_6D_6) δ 1.30 (8H, m, $^3J_{HH} = 6.6$ Hz, CH_2 , THF), 1.66 (18H, s, ArC-C(CH_3) $_3$), 1.96 (6H, m, N- $CH_2\{CH_2\}CH_2$ -N), 2.41 (6H, s, ArC- CH_3), 2.75 (4H, m, N- CH_2CH_2 -N), 3.51 (8H, m, $^3J_{HH} = 6.6$ Hz, CH_2 , THF), 3.61 (4H, s, ArC- CH_2 -N), 6.85 (2H, d, $^2J_{HH} = 2.3$ Hz, ArH), 7.35 (2H, d, $^2J_{HH} = 2.3$ Hz, ArH). ^{13}C { 1H } NMR (300 MHz, 298 K, C_6D_6) δ 21.6 (ArC- CH_3), 25.8 (CH_2 , THF), 27.7 (N- $CH_2\{CH_2\}CH_2$ -N), 30.8 (ArC-C-(CH_3) $_3$), 35.4 (ArC-C-(CH_3) $_3$), 51.1 (N- CH_2CH_2 -N), 53.5 (N- $CH_2\{CH_2\}CH_2$ -N), 62.2 (ArC- CH_2 -N), 68.5 (CH_2 , THF), 120.4 (ArC- CH_2 -N), 126.5 (ArCH), 131.3 (ArC- CH_3), 137.6 (ArC-C-(CH_3) $_3$), 164.5 (ArC-O). 7Li { 1H } NMR (C_6D_6 , 298 K, δ) 1.60. MS (MALDI-TOF) m/z (% ion): 464.3 (100, $Li_2[N_2O_2^{BuMePip}]^{+}$).

Synthesis of 4 This was prepared in a similar manner to **2** to yield (2.02 g, 96%) of a yellow product. Anal. calc'd for $C_{29}H_{42}Na_2N_2O_2$: C, 70.13; H, 8.52; N, 5.64. Found: C, 55.94; H, 9.76; N, 3.90. 1H NMR (300 MHz, 298 K, C_6D_6) δ 1.25 (8H, m, $^3J_{HH} = 6.7$ Hz, CH_2 , THF), 1.73 (18H, s, ArC-C(CH_3) $_3$), 2.34 (6H, s, ArC- CH_3), 2.99 (4H, br, N- $CH_2\{CH_2\}CH_2$ -N), 3.25 (8H, m, $^3J_{HH} = 6.7$ Hz, CH_2 , THF), 4.09 (4H, br, ring NCH_2Ar), 6.83 (2H, s, ArH), 7.23 (2H, s, ArH). 1H NMR (500 MHz, 298 K, C_5D_5N) δ 1.16 (6H, s, CH_2 , THF), 1.59 (18H, s, ArC-C(CH_3) $_3$), 1.95 (2H, s, N- $CH_2\{CH_2\}CH_2$ -N), 2.24 (4H, m, N- $CH_2\{CH_2\}CH_2$ -N), 2.45 (6H, s, ArC- CH_3), 2.94 (4H, m, N- CH_2CH_2 -N), 3.28 (2H, s, NCH_2Ar), 3.58 (2H, s, CH_2 , THF), 4.40 (2H, s, NCH_2Ar),

6.97 (2H, s, ArH), 7.30 (2H, s, ArH). ^{13}C $\{^1\text{H}\}$ NMR (300 MHz, 298 K, CDCl_3) δ 20.96 (ArC- CH_3), 25.78 (CH_2 , THF), 26.98 (N- $\text{CH}_2\{\text{CH}_2\}\text{CH}_2\text{-N}$), 29.72 (ArC-C-(CH_3) $_3$), 34.74 (ArC-C-(CH_3) $_3$), 53.20 (N- $\text{CH}_2\text{CH}_2\text{-N}$), 54.66 (N- $\text{CH}_2\{\text{CH}_2\}\text{CH}_2\text{-N}$), 62.12 (ArC- $\text{CH}_2\text{-N}$), 68.13 (CH_2 , THF), 122.12 (ArC- $\text{CH}_2\text{-N}$), 126.90 (ArCH), 127.47 (ArCH), 136.55 (ArC-C-(CH_3) $_3$), 154.41 (ArC-O). MS (MALDI-TOF) m/z (% ion): 497.2 (10, $\text{Na}_2[\text{N}_2\text{O}_2^{\text{BuMePip}}]^{++}$). 475.2 (25, $\text{Na}[\text{N}_2\text{O}_2^{\text{BuMePip}}]^{+}$).

X-ray Crystallography

Crystals of **1** and **4** were mounted on low temperature diffraction loops. All measurements were made on a Rigaku Saturn70 CCD diffractometer using graphite monochromated Mo-K α radiation, equipped with a SHINE optic. A summary of the collection details and refinement results can be found in Table S1. For both structures, H-atoms were introduced in calculated positions and refined on a riding model while all non-hydrogen atoms were refined anisotropically. While refinement of **4** proceeded normally, in the structure of **1**, two disordered *t*-butyl groups were present ([C60-C62] and [C63-65] with respective occupancies 0.647(14):0.353(14), and [C67-69] and [C70-72] with respective occupancies 0.761(10):0.239(10).) Similar anisotropic restraints were applied to these groups, as well as to one THF molecule (O5, C77-C80). Further disorder was treated by the Platon⁸⁶ Squeeze procedure which was applied to recover 119 electrons per unit cell in two voids (total volume 813 \AA^3); that is 59.5 electrons per formula unit. Disordered lattice solvent toluene molecules (50 electrons per C_7H_8 ; one molecule per formula unit) were present prior to the application of Squeeze, however, a satisfactory point atom model could not be achieved. Note that there are two well-ordered toluene molecules associated with each formula unit that were not removed from the model using Squeeze.

Crystal Data for 1: $\text{C}_{103}\text{H}_{156}\text{Li}_4\text{N}_4\text{O}_7$ ($M=1590.15$ g/mol), triclinic, space group P-1 (no. 2), $a = 16.592(2)$ \AA , $b = 18.655(2)$ \AA , $c = 19.067(2)$ \AA , $\alpha = 103.219(7)^\circ$, $\beta = 98.581(7)^\circ$, $\gamma = 109.095(8)^\circ$, $V = 5265.8(10)$ \AA^3 , $Z = 2$, $T = 163(2)$ K, $\mu(\text{MoK}\alpha) = 0.061$ mm^{-1} , $D_{\text{calc}} = 1.003$ g/cm^3 , 43063 reflections measured ($6^\circ \leq 2\theta \leq 53^\circ$), 21429 unique ($R_{\text{int}} = 0.0454$) which were used in all calculations. The final R_1 was 0.1130 ($>2\sigma(I)$) and wR_2 was 0.3597 (all data). CCDC no. 1410026

Crystal Data for 4: C₆₆H₁₀₀N₄Na₄O₆ ($M=1137.45$ g/mol), monoclinic, space group P2₁/n (no. 14), $a = 12.898(4)$ Å, $b = 13.741(4)$ Å, $c = 18.695(6)$ Å, $\beta = 101.518(4)^\circ$, $V = 3246.7(17)$ Å³, $Z = 2$, $T = 163$ K, $\mu(\text{MoK}\alpha) = 0.096$ mm⁻¹, $D_{\text{calc}} = 1.164$ g/cm³, 24304 reflections measured ($4.61^\circ \leq 2\theta \leq 54.206^\circ$), 7155 unique ($R_{\text{int}} = 0.0374$) which were used in all calculations. The final R_1 was 0.0543 ($I > 2\sigma(I)$) and wR_2 was 0.1653 (all data). CCDC no. 1410027

Polymerization Procedures

Typical Bulk Polymerization Procedure: A monomer:initiator ratio employed was 100:1 and the reactions were conducted at 130 °C. A Schlenk tube equipped with magnetic stir bar was charged in a glovebox with the required amount of LA (0.50 g, 3.5 mmol) and initiator (0.02-0.023 g, 0.035 mmol). The reaction vessel was sealed, brought out of the glovebox and immersed in an oil bath that was preheated to 130 °C. At the desired time an aliquot was withdrawn from the flask for ¹H NMR analysis to determine the monomer conversion. The vial was then placed in an ice bath to halt the reaction and solidify the polymer. The resulting solid was dissolved in dichloromethane and the polymer, precipitated with acidified methanol. Centrifugation was applied where needed for better separation of the solids. Solvents were decanted and the white solids were dried *in vacuo* followed by drying in a vacuum oven at 40 °C overnight.

Typical Solution Polymerization Procedure: The reaction mixtures were prepared in a glovebox and subsequent operations were performed with standard Schlenk techniques. A Schlenk tube containing a stir bar and the monomer (0.85 g, 5.9 mmol) in solvent (CH₂Cl₂, Toluene or THF) was prepared. A second Schlenk tube was prepared containing a stir bar and the catalyst (0.007-0.0085 g, 0.0118 mmol) and a solution of BnOH (127 μL, 0.0118 mmol), if appropriate in 10 mL of solvent (CH₂Cl₂, Toluene). Then the lactide solution was transferred by cannula to the complex mixture. Timing of the reaction began when all the lactide was transferred. An aliquot of the reaction solution was taken for NMR spectroscopic analysis, and the reaction was quenched immediately by the addition of methanol. The resulting solid was dissolved in dichloromethane and the polymer precipitated with excess cold methanol. Solvents were decanted and the white solids were dried *in vacuo* followed by drying in a vacuum oven at 40 °C overnight.

Conclusions

In conclusion, we have prepared and characterized tetrametallic lithium and sodium amine-bis(phenolate) complexes. At room temperature, these complexes demonstrate good activity for ring-opening polymerization of *rac*-lactide both in the absence and presence of benzyl alcohol to yield polymers with narrow dispersities. The effect of solvents on the ROP reactions was studied. The sodium complexes outperform their lithium analogues especially in the presence of BnOH. We note that the effect of BnOH on the lithium initiators is negligible. The molecular weight of PLAs can be tuned according to the monomer:alcohol ratio, where increasing the amount of BnOH results in proportionally lower molecular weight polymers. GPC data of the produced polymers point to well-controlled polymerizations but evidence for transesterification is seen in mass spectra of the polymers. On the basis of stoichiometric model reactions the polymerization occurs via a coordination-insertion mechanism.

Acknowledgements

NSERC of Canada, Memorial University, RDC-NL and CFI are thanked for operating and instrument grants. Special thanks to the Saudi Arabian Cultural Bureau in Canada and Taif University (Saudi Arabia) for financial support. We thank Yann Sarazin (Université de Rennes 1) for valuable suggestions and Céline Scheider (Memorial University) for assistance with NMR experiments.

References:

1. M. M. Reddy, S. Vivekanandhan, M. Misra, S. K. Bhatia and A. K. Mohanty, *Prog. Polym. Sci.*, 2013, **38**, 1653-1689.
2. M. Singhvi and D. Gokhale, *RSC Adv.*, 2013, **3**, 13558– 13568.
3. A. Arbaoui and C. Redshaw, *Polym. Chem.*, 2010, **1**, 801-826.
4. B. Gupta, N. Revagade and J. Hilborn, *Prog. Polym. Sci.*, 2007, **32**, 455-482.
5. C. K. Williams, *Chem. Soc. Rev.*, 2007, **36**, 1573–1580.
6. S. Slomkowski, S. Penczek and A. Duda, *Polym. Adv. Technol.*, 2014, **25**, 436-447.
7. M. J. Stanford and A. P. Dove, *Chem. Soc. Rev.*, 2010, **39**, 486-494.
8. R. H. Platel, L. M. Hodgson and C. K. Williams, *Polym. Rev.*, 2008, **48**, 11–63.

9. A. –C. Albertsson and I. K. Varma, *Biomacromolecules*, 2003, **4**, 1466-1486.
10. J. W. Rhim, H. M. Park and C. S. Ha, *Prog. Polym. Sci.*, 2013, **38**, 1629–1652.
11. I. Armentano, N. Bitinis, E. Fortunati, S. Mattioli, N. Rescignano, R. Verdejo, M. A. L. Manchado and J. M. Kenny, *Prog. Polym. Sci.*, 2013, **38**, 1720–1747.
12. R. A. Auras, B. Harte, S. Selke and R. Hernandez, *J. Plast. Film Sheeting*, 2003, **19**, 123-135.
13. Y. Ohya, A. Takahashi and K. Nagahama, *Adv. Polym. Sci.*, 2012, **247**, 65-114.
14. K. Hamad, M. Kaseem, H. W. Yang, F. Deri and Y. G. Ko, *Polym. Lett.*, 2015, **9**, 435-455.
15. O. Wichmann, R. Sillanpaa and A. Lehtonen, *Coord. Chem. Rev.*, 2012, **256**, 371-392.
16. C. A. Wheaton, P. G. Hayes and B. J. Ireland, *Dalton Trans.*, 2009, **38**, 4832–4846.
17. W. Yi and H. Ma, *Dalton Trans.*, 2014, **43**, 5200-5210.
18. J. P. Davin, J. C. Buffet, T. P. Spaniol and J. Okida, *Dalton Trans.*, 2012, **41**, 12612–12618.
19. E. L. Marshall, V. C. Gibson and H. S. Rzepa, *J. Am. Chem. Soc.*, 2005, **127**, 6048–6051.
20. L. Wang and H. Ma, *Macromolecules*, 2010, **43**, 6535–6537.
21. J. Ejfler, S. Szafert, K. Mierzwicki, L. B. Jerzykiewicz and P. Sobota, *Dalton Trans.*, 2006, 6556-6562.
22. W. C. Hung and C. C. Lin, *Inorg. Chem.*, 2009, **48**, 728-734.
23. Y. Sarazin, V. Poirier, T. Roisnel and J. F. Carpentier, *Eur. J. Inorg. Chem.*, 2010, **22**, 3423-3428.
24. A. D. Schofield, M. L. Barros, M. G. Cushion, A. D. Schwarz and P. Mountford, *Dalton Trans.*, 2009, 85-96.
25. X. Zhang, T. J. Emge and K. C. Hultsch, *Organometallics*, 2010, **29**, 5871-5877.
26. H-Y Chen, L. Mialon, K. A. Abboud and S. A. Miller, *Organometallics*, 2012, **31**, 5252-5261.
27. D. J. Darensbourg, W. Choi, O. Karroonnirun and N. Bhuvanesh, *Macromolecules*, 2008, **41**, 3493-3502.
28. B. Liu, T. Roisnel, J.-P. Guégan, J.-F. Carpentier and Y. Sarazin, *Chem- Eur. J.*, 2012, **18**, 6289-6301.

29. B. Gao, R. L. Duan, X. Pang, X. Li, Z. Qu, Z. H. Tang, X. L. Zhuang and X. S. Chen, *Organometallics*, 2013, **32**, 5435-5444.
30. Z. Qu, R. Duan, X. Pang, B. Gao, X. Li, Z. Tang, X. Wang, X. Chen, *Polym. Chem.*, 2014, **52**, 1344-1352.
31. X. Pang, R. L. Duan, X. Li and X. S. Chen, *Polym. Chem.*, 2014, **5**, 3894–3900.
32. L. Postigo, M. C. Maestre, M. E. G. Mosquera, T. Cuenca and G. Jiménez, *Organometallics*, 2013, **32**, 2618-2624.
33. N. Ikpo, S. M. Barbon, M. W. Drover, L. N. Dawe and F. M. Kerton, *Organometallics*, 2012, **31**, 8145-8158.
34. M. O. Miranda, Y. Deporre, H. V-Lima, M. A. Johnson, D. J. Marell, C. J. Cramer and W. B. Tolman, *Inorg. Chem.*, 2013, **52**, 13692-13701.
35. R. K. Dean, A. M. Reckling, H. Chen, L. N. Dawe, C. M. Schneider and C. M. Kozak, *Dalton Trans.*, 2013, **42**, 3504-3520.
36. S-C. Rosca, D-A. Rosca, V. Dorcet, C. M. Kozak, F. M. Kerton, J-F. Carpentier and Y. Sarazin, *Dalton Trans.*, 2013, **42**, 9361-9375.
37. N. Ikpo, C. Hoffmann, L. N. Dawe and F. M. Kerton, *Dalton Trans.*, 2012, **41**, 6651-6660.
38. Y. Huang, Y.-H. Tsai, W.-C. Hung, C.-S. Lin, W. Wang, J.-H. Huang, S. Dutta and C.-C. Lin, *Inorg. Chem.*, 2010, **49**, 9416-9425.
39. L. Wang, X. B. Pan, L. H. Yao, N. Tang and J. C. Wu, *Eur. J. Inorg. Chem.*, 2011, **41**, 632-636.
40. C.-A. Huang, C.-L. Ho and C.-T. Chen, *Dalton Trans.*, 2008, 3502-3510.
41. C.-A. Huang and C.T. Chen, *Dalton Trans.*, 2007, 5561-5566.
42. F. M. Kerton, C. M. Kozak, K. Lüttgen, C. E. Willans, R. J. Webster and A. C. Whitwood, *Inorg. Chim. Acta.*, 2006, **359**, 2819-2825.
43. B.-T. Ko and C.-C. Lin, *J. Am. Chem. Soc.*, 2001, **123**, 7973-7977.
44. W. Clegg, M. G. Davidson, D. V. Graham, G. Griffen, M. D. Jones, A. R. Kennedy, C.T. O'Hara, L. Russo and C. M. Thomson, *Dalton Trans.*, 2008, 1295-1301.
45. Z. Janas, T. Nerkowski, E. Kober, L. B. Jerzykiewicz and T. Lis, *Dalton Trans.*, 2012, **41**, 442-447.

46. E. Kober, R. Petrus, P. Kocięcka, Z. Janas and P. Sobota, *Polyhedron*, 2015, **85**, 814-823.
47. F. M. G-Valle, R. Estivill, C. Gallegos, T. Cuenca, M. E. G. Mosquera, V. Tabertero and J. Cano, *Organometallics*, 2015, **34**, 477-487.
48. W.-Y. Lu, M.-W. Hsiao, S. C. N. Hsu, W.-T. Peng, Y.-J. Chang, Y.-C. Tsou, T.-Y. Wu, Y.-C. Lai, Y. Chen and H.-Y. Chen, *Dalton Trans.*, 2012, **41**, 3659–3667.
49. X. Xu, X. Pan, S. Tang, X. Lv, L. Li, J. Wu and X. Zhao, *Inorg. Chem.*, 2013, **29**, 89-93.
50. B. Calvo, M. G. Davidson and D. G-Vivó, *Inorg. Chem.*, 2011, **50**, 3589-3595.
51. X. Xu, Y. Yao, Y. Zhang and Q. Shen, *Inorg. Chem.*, 2007, **46**, 3743-3751.
52. Nduka Ikpo, PhD Thesis, Memorial University of Newfoundland, 2012.
53. S. L. Hancock, R. Gati, M. F. Mahon, E. Y.Tshuva and M. D. Jones, *Dalton Trans.*, 2014, **43**, 1380-1385.
54. S. L. Hancock, M. F. Mahon and M. D. Jones, *Chem. Cent. J.*, 2013, **7**, 135.
55. S. L. Hancock, M. F. Mahon and M. D. Jones, *Dalton Trans.*, 2011, **40**, 2033-2037.
56. J. Baldamus and E. Hecht, *Z. Anorg. Allg. Chem.*, 2003, **629**, 188-191.
57. M. Sankaralingam and M. Palaniandavar, *Dalton Trans.*, 2014, **43**, 538-550.
58. S. L. Hancock, M. D. Jones, C. J. Langridge and M. F. Mahon, *New J. Chem.*, 2012, **36**, 1891– 1896.
59. S. L. Hancock, M. F. Mahon, G. K-Kohn and M. D. Jones, *Eur. J. Inorg. Chem.*, 2011, **29**, 4596-4602.
60. R. Mayilmurugan, B. N. Harum, M. Volpe, A. F. Sax, M. Palaniandavar and N. C. M-Zanetti, *Chem. Eur. J.*, 2011, **17**, 704-713.
61. L. L. Mendes, C. Fernandes, R. W. A Franco, L. M. Lube, S-H. Wei, J. H. Reibenspies, D. J. Darensbourg and A. H. Jr, *J. Braz. Chem. Soc.*, 2014, **25**, 1050-1061.
62. R. Mayilmurugan, M. Sankaralingam, E. Suresh and M. Palaniandavar, *Dalton Trans.*, 2010, **39**, 9611-9625.
63. R. Mayilmurugan, H. S-Evans, E. Suresh and M. Palaniandavar, *Dalton Trans.*, 2009, **26**, 5101-5114.
64. A. W. Addison, T. N. Rao, J. Reedijk, J. Van Rijn and G. C. Verschoor, *J. Chem. Soc., Dalton Trans.*, 1984, 1349-1356.

65. S. Uhlenbrock, R. Wagner and B. Krebs, *J. Chem. Soc., Dalton Trans.*, 1996, 3731-3736.
66. G. Murphy, C.O. Sullivan, B. Murphy and B. Hathaway, *Inorg. Chem.*, 1998, **37**, 240-248.
67. D. S. Marlin, M. M. Olmstead and P. K. Mascharak, *Inorg. Chem.*, 2001, **40**, 7003-7008.
68. A. Macchioni, G. Ciancaleoni, C. Zuccaccia and D. Zuccaccia, *Chem. Soc. Rev.*, 2008, **37**, 479-489.
69. M.W. Drover, J. N. Murphy, J. C. Flogeras, C. M. Schneider, L. N. Dawe and F. M. Kerton, *Polyhedron*, 2015, doi:10.1016/j.poly.2015.07.071.
70. R. E. Drumright, P. R. Gruber and D. E. Henton, *Adv. Mater.*, 2000, **12**, 1841-1846.
71. C. Paetz and R. Hagen, *Chem. Ing. Tec.*, 2014, **86**, 519-523.
72. S. Bian, S. Abbina, Z. Lu, E. Kolodka and G. Du, *Organometallics*, 2014, **33**, 2489-2495.
73. K. D.-Pressing, J. H. Lehr, M. E. Pratt, L. N. Dawe, A. A. Sarjeant and C. M. Kozak, *Dalton Trans.*, 2015, 44, 12365-12375.
74. N. Ikpo, L. N. Saunders, J. L. Walsh, J. M. B. Smith, L. N. Dawe and F. M. Kerton, *Eu. J. Inorg. Chem.*, 2011, 5347-5359.
75. N. Ajellal, J.-F. Carpentier, C. Guillaume, S. M. Guillaume, M. Hérou, V. Poirier, Y. Sarazin and A. A. Trifonov, *Dalton Trans.*, 2010, **39**, 8363-8376.
76. K. A. M. Thakur, R. T. Kean, E. S. Hall, J. J. Kolstad, T. A. Lindgren, A. M. Doscotch, J. I. Siepmann and E. J. Munson, *Macromolecules*, 1997, **30**, 2422-2428.
77. M. H. Thibault and F. G. Fontaine, *Dalton Trans.*, 2010, **39**, 5688.
78. N. Maudoux, T. Roisnel, J.-F. Carpentier and Y. Sarazin, *Organometallics*, 2014, **33**, 5740-5748.
79. M. A. Sinenkov, G. K. Fukin, A. V. Cherkasov, N. Ajellal, T. Roisnel, F. M. Kerton, J.-F. Carpentier and A. A. Trifonov, *New J. Chem.*, 2011, **35**, 204-212.
80. C. E. Willans, M. A. Sinenkov, G. K. Fukin, K. Sheridan, J. M. Lynam, A. A. Trifonov and F. M. Kerton, *Dalton Trans.*, 2008, **19**, 3592-3598.
81. A. K. Sutar, T. Maharana, S. Dutta, C.-T. Chen and C.-C. Lin, *Chem. Soc. Rev.*, 2010, **39**, 1724-1746.
82. H. E. Dyer, S. Huijser, A. D. Schwarz, C. Wang, R. Duchateau and P. Mountford, *Dalton Trans.*, 2008, 32-35.

83. T. L. Yu, B. H. Huang, W. C. Hung, C. C. Lin, T. C. Wang and R. M. Ho, *Polymer*, 2007, **48**, 4401-4411.
84. H. Kato, T. Saito, M. Nabeshima, K. Shimada and S. Kinugasa, *J. Magn. Reson.*, 206, **180**, 266–273.
85. D. Zuccaccia and A. Macchioni, *Organometallics*, 2005, **24**, 3476-3486.
86. A. L. Spek, *J. Appl. Cryst.*, 2003, **36**, 7-13.

For Table of Contents Entry Only:

Sodium complex contains interesting intramolecular η^6 -arene interaction and shows excellent catalytic behaviour for polymerization of lactide.

